의학박사 학위논문

Assessment of a cellular immune response from peripheral blood of non-human primate after porcine islet xenotransplantation

말초혈액을 이용한 영장류 췌도이종이식에서의 세포성 면역 반응 측정

2017년 2월

서울대학교 대학원

의과학과 의과학전공

김 현 제

A thesis of the Degree of Doctor of Philosophy

말초혈액을 이용한 영장류 췌도이종이식에서의 세포성 면역 반응 측정

Assessment of a cellular immune response from peripheral blood of non-human primate after porcine islet xenotransplantation

February 2017

Major in Biomedical Sciences
Department of Biomedical Sciences
Seoul National University Graduate School
Hyun-Je Kim

말초혈액을 이용한 영장류 췌도이종이식에서의
세포성 면역 반응 측정

지도 교수 박정규

이 논문을 의학박사 학위논문으로 제출함

2017년 2월

서울대학교 대학원

의과학과 의과학전공

김 현 제

김현제의 의학박사 학위논문을 인준함

2017년 2월

위 원 장 _____ (인)

부위원장 _____ (인)

위 원 _____ (인)
위 원 _____ (인)
위 원 _____ (인)

Assessment of a cellular immune response from peripheral blood of non-human primate after porcine islet xenotransplantation

by
Hyun-Je Kim

A thesis submitted to the Department of Biomedical Sciences in partial fulfillment of the requirements for the Degree of Doctor of Philosophy in Medical Science at Seoul National University

February 2017

Approved by Thesis Committee:

Professor _____Chairman

Professor _____ **Vice chairman**

Professor _____

Professor _____

Professor _____

ABSTRACT

Introduction: Outstanding results from nonhuman primate study put islet xenotransplantation with immunosuppression closer to the clinical application. To establish successful immune suppressive protocols, immune monitoring by which the fate of graft could be predictable would be critical. However, there are few reports showing predictive immune parameters associated with the fate of the graft in pig to nonhuman primate islet xenotransplantation model. Implementation of an appropriate monitoring method to detect the development of detrimental porcine antigen-specific cellular immune responses is also necessary. In addition, clarifying the causes of islet death in the chronic phase after islet transplantation is important.

Methods: Porcine islets were transplanted to diabetic nonhuman primate under immunosuppression. During the observation period, the number and ratio of T cell subsets were analyzed by flow cytometry from peripheral blood of seven-teen transplanted monkeys to find out graft-fate predictive immune parameters. To find out the optimal ELISpot assay conditions, the numbers of responder and stimulator cells were determined. Then, ELISpot assays were

conducted on serial stocks of the peripheral blood mononuclear cell (PBMC) samples previously isolated from four NHP recipients transplanted with porcine islets to validate the essay's utility to monitor the porcine antigen-specific cellular immune responses. Either splenocytes from donor pigs or pancreatic islets from third-party pigs were also used for antigen stimulation. Furthermore, I performed RNA sequencing with peripheral blood and bioinformatics analysis in two monkeys as a way to find out or predict potential cause(s) of graft failure after 100 days after transplantation.

Results: After the depletion of $CD3^+$ T cells with rATG with immunosuppression, the mean recovery time of $CD3^+$ T cells was 38.2 ± 47.7 days. $CD4^+$ T cells were the dominant populations in $CD3^+$ T cells before the anti-thymocyte globulin treatment. However, $CD8^+CD28^-CD95^+$ effector memory T cell's rapid expansion reversed the ratio of $CD4^+$ versus $CD8^+$ T cells. T lymphocyte subtype analysis with graft survival day revealed that $CD4^+/CD8^+$ T cell ratio was significantly associated with early graft failure.

The optimal conditions for the ELISpot assay were defined as 2.5×10^5 responder cells incubated with 5.0×10^5 stimulator cells in 96-well, flat-bottom plates without further co-stimulation. Using donor splenocytes as stimulators, a serial interferon-gamma (IFN-γ) ELISpot assay with PBMCs from the monkeys with prolonged porcine islet grafts (>180 days) demonstrated that the number of donor antigen (not islet-specific)-specific IFN-γ-producing cells significantly increased upon overt graft rejection. By using novel bioinformatics tool, I found that highly relevant activated

'immunologic' pathways were indeed manifest in graft failed animal compared with control one in chronic phase. In line with this notion, I further confirmed that the porcine islets were heavily infiltrated with $CD3^+$ T cells by immunohistochemistry on biopsied liver samples.

Conclusions: $CD4^+/CD8^+$ T cell ratio could be used as a surrogate marker to predict early graft failure in porcine islet xenotransplantation in NHPs with immunosuppression. I also showed that the use of recipient PBMCs in a porcine antigen-specific IFN-γ ELISpot assay is a reliable method for monitoring T-cell-mediated rejection in pig-to-NHP islet xenotransplantation. I further demonstrated that a new bioinformatics analysis combined with peripheral RNA sequencing could unveil insidious immune rejection in the chronic phase after pig-to-NHP islet xenotransplantation.

* This work is partly published in American Journal of Transplantation (Shin JS, Kim JM, Kim JS, Min BH, Kim YH, Kim HJ et at. Long-term control of diabetes in immunosuppressed nonhuman primates (NHP) by the transplantation of adult porcine islets. American Journal of Transplantation. 2015;15:2837-50), Xenotransplantation (Kim JM, Shin JS, Min BH, Kim HJ, Kim JS, Yoon IH et al. Induction, management, and complications of streptozotocin-induced diabetes mellitus in rhesus monkeys. Xenotransplantation. 2016; 23: 472-78) and Xenotransplantation (Kim HJ, Yoon IH, Min BH, Kim HY, Shin JS, Kim JM et al. Porcine antigen-specific IFN-γ ELISpot as a potentially valuable tool for monitoring cellular immune responses in pig to non-human primate islet xenotransplantation. Xenotransplantation. 2016; 23(4): 310-9). A part of this work is currently submitted in Xenotransplantation (Shin JS, Ki JM, Min BH, Yoon IH, Kim HJ, Kim JS et al. Pre-clinical results in pig-to-nonhuman primate islet xenotransplantation using anti CD40 antibody based immunosuppression. Xenotransplantation. Manuscript ID: XENO-16-O-0082), planned to submitted in Xenotransplantation (Kim HJ, Yoon IH, Kim JS, Nam HY, Min BH, Shin JS, et al. $CD4^+/CD8^+$ T cell ratio as a predictive marker for early graft failure in pig to non-human primate islet xenotransplantation with

immunosuppression and Nature communications (Kim HJ, Moon JH, Shin JS, Kim B, Kim JS, Min BH et al. Bioinformatics analysis combined with peripheral blood RNA-sequencing unveiled insidious immune rejection in the chronic phase after pig-to-nonhuman primate islet xenotransplantation.

Keywords: Islet transplantation, Porcine, Xenotransplantation, Non-human primate, Cellular immune monitoring, Enzyme-linked immunosorbent spot assay (ELISpot), RNA seq., Bioinformatics

Student number: 2012-30577.

CONTENTS

LIST OF TABLES AND FIGURES

General Material, Methods and Results

Part 1

Part 2

Part 3

LIST OF ABBREVIATIONS

rATG: rabbit anti-thymocyte globulin

NHP: non-human primate

PBMCs: peripheral blood mononuclear cells

MFI: Mean fluorescence intensity

ELISpot: enzyme-linked immunosorbent spot

DPT: days post transplantation

ELISA: Enzyme-linked immunosorbent assay

FACS: fluorescence activated cell sorting

TRAP: Time-series RNA-seq analysis package

RNA-seq: RNA-sequencing

GLPAPs: Graft loss period-related activated pathways

GENERAL INTRODUCTION

A lot of historical surgeon's efforts combined with the invention of immunosuppression opened the era of clinical organ transplantation in 20th century[1]. However, there have been two important hurdles which should be overcome in this field. There are shortage of donor organ[2,3] and adverse effects of immunosuppression[4]. To vanquish the first arm of an obstacle, biomedical scientists have actively studied stem cells[5], xenotransplantation[6] and bio-artificial organs[7]. The latter arm of obstacle is believed to be controlled by the induction of donor-specific immune tolerance[8] or induced pluripotent stem cell technology[9]. However, although many efforts were put forward to solve these problems, none of them have been successfully adopted in routine clinical practice yet.

Transplanted grafts were inevitably deteriorated by the host immune system. Host immune response to the graft could be classified either by time of happening or responsible host immune elements. Hyper-acute rejections which following transplantation within minutes to hours are mainly due to the pre-formed antibody to the grafts[10]. These hyper-acute rejections were traditionally the most important barrier of xenotransplantation as human possess pre-formed anti-Gal antibody[11] which could fixate complements on pig organs. However, brilliant advancement of gene-editing technology developed Gal-Knock out pig[12] in 2002 and enable us to go beyond the hurdle of hyper-acute rejection.

Acute rejections were generally considered to begin several days to a few weeks after the transplantation. Main host elements of the immune system were divided into the cellular and humoral compartment. If the main players are the cellular portions, I call

the events acute cellular rejection. On the other hands, if the main contributors belong to the humoral compartments, I call them acute humoral rejection. The latter is mainly caused by donor antigen-specific antibody. There are a lot of reports measuring donor-specific antibody to monitor and predict the acute humoral rejection at various transplant including kidney, liver, heart and pancreas transplantation[13-17]. These acute antibodies mediated rejections were generally confirmed by demonstrating the complement fixation in tissue biopsy sample of grafts. Acute cellular mediated rejections were histologically defined as infiltration of T cell inside of the grafts. These T cells could be $CD8^+$ cytotoxic T cells which could kill the graft directly with perforin and granzyme or $CD4^+$ helper T cells which help recruiting and activating other immune cells. Different from antibody mediated rejections which can be monitored by measuring donor-specific antibodies, I don't have valuable tools in my hands to look into these cell-mediated immune rejections.

Chronic rejections develop insidiously during months or years[18]. Unlike hyper-acute and acute rejection, chronic rejections of different organ or tissue transplants show different pathology from each other. This implies that pathophysiology of chronic rejections are still obscure.

To prevent an immune response to the grafts described above, the monitoring of immune response to the donor grafts after the transplantation is a very important issue in clinical transplantation. Hence, apart from monitoring humoral immune response in which powerful donor-specific antibody measurement already exists, I decided to study 1) the tools of monitoring the cellular immune response and 2) clarifying the cause of chronic phase graft loss in porcine islet xenotransplantation by using non-human primate model.

Strategies to find out the tools for monitoring of cellular immune responses could be subcategorized into searching immune activation biomarkers and regulatory immune cells[19]. A lot of regulatory immune cells including $CD4^+$ T cells, B cells, macrophages and so on after the transplantation were figured out so far[20]. Among them, I paid attention to the number of T cells after the transplantation to develop novel biomarkers of monitoring the cellular immune response after the porcine islet xenotransplantation with immunosuppression as their role in renal transplant recipients were recently reported[21]. Hence, I decided to check time-series of functional T cell subset's number of seven-teen graft recipient monkeys.

Immune activation biomarkers were further able to be divided into checking donor-specific reactivity and donor non-specific reactivity. Because enumerating the antigen-specific T cell clone in peripheral blood is more accurate method to reflect graft specific cellular immune response, I decided to establish standardized method of antigen-specific IFN-γ Enzyme linked immunosorbent assay (ELISpot) in porcine islet NHP xenotransplantation by using four graft recipient monkeys which experienced similar immunosuppression protocols.

If I contemplate the complexity of immune response in vivo, searching for single gene, surface molecules, cell types which are responsible for graft specific cellular immune response might be absurd. In reality, Khatri et al. demonstrated that not only single gene but several gene sets could predict the prognosis of the grafts[22,23]. In these perspectives, I decided to gather the RNAseq. data from peripheral blood of two graft recipient monkeys, one of which experienced chronic graft failure. I expected that I was able to find out the cause of chronic graft loss by using bioinformatics analysis of RNAseq. data.

General Material, Methods and Results

1. Animals

Total 17 rhesus monkeys (*Macaca mulatta*) were used in this study. R051, R080, R082, R084, R089, R086, R088, R091, R095, R092, R087, R008, R131, R143, R147, R144 and R130 were used in my experiments. All procedures were carried out in compliance with the guidelines set forth in the *Guide for the Care and Use of Laboratory Animals* prepared by the Institute of Laboratory Animal Resources and published by the National Institutes of Health (NIH Publication No. 86-23, revised 2011), and approved by the Seoul National University Institutional Animal Care and Use Committee (IACUC no. 15-0297-S1A0). Islet donor pigs, Seoul National University (SNU) miniature pigs were bred and maintained in a barrier-sustained and specific pathogen-free facility.

2. Porcine islet isolation

Porcine islets were isolated as previously described[24] (Fig.1.). Briefly, islet isolation was performed using the modified Ricordi method after pancreatectomy. The harvested pancreas was distended using a preservation solution containing Liberase MTF C/T (Roche Diagnostics, Indianapolis, IN) or CIzyme™ collagenase and CIzyme™ BP protease (VitaCyte, Indianapolis, IN, USA).

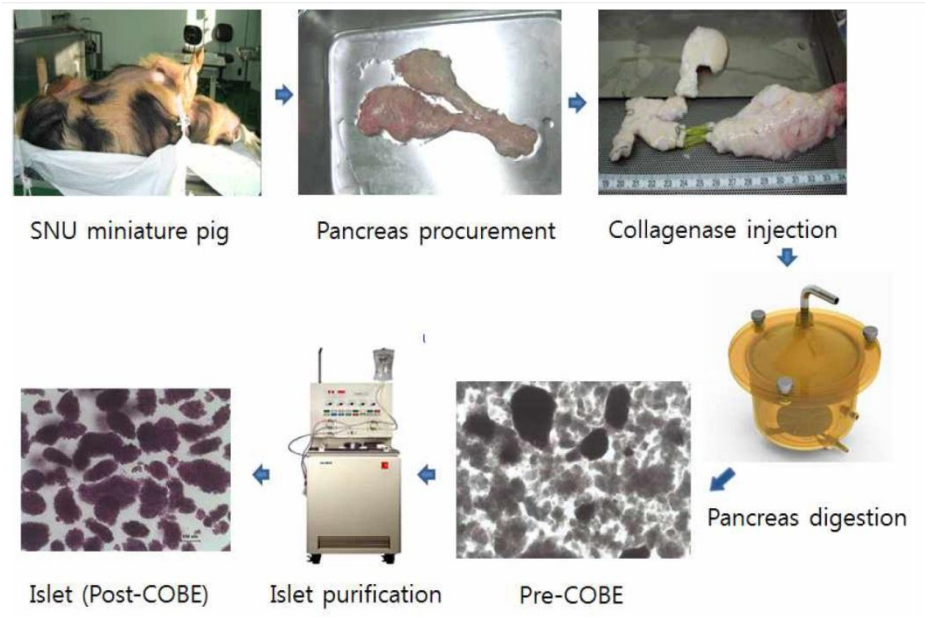

Fig. 1. Procedures for porcine islet isolation. Islet isolation was performed using SNU minipig. After pancreatectomy, the harvested pancreas was distended by injection of collagenase. Islets were purified by density gradient separation method using poly-sucrose solution.

3. Induction of diabetes in NHPs

Diabetes induction and islet transplantation were conducted as previously described[24,25]. A central venous catheter (5Fr. Dual-Lumen PICC; Bard Access Systems, Salt Lake City, UT, USA) was inserted into the right internal jugular vein in monkeys under general anesthesia. Monkeys were fasted overnight and were pre-hydrated with normal saline (NS; 0.9% NaCl, 5 mL/kg/h intravenously) via a tether system for 12 hours before STZ (Sigma–Aldrich, St Louis, MO, USA) administration to reduce adverse nephrotoxic effects. A high dose of STZ (110 mg/kg) was diluted with 10 mL normal saline and given intravenously within 10 min at 4 pm to prevent hypoglycemia at 9 am

in next day. Because maximum nadir of hypoglycemia usually occurs about 17 hours after STZ injection, 5% dextrose solution (5 DS) was infused at 1 hour after STZ injection to prevent hypoglycemia and nephrotoxicity.

4. Islet transplantation into NHPs

All monkeys fasted for 12 h before surgery. A laparotomy was performed, and the jejunal arch was exposed to infuse the islets (Fig.2). A 24- or 22-gauge catheter was inserted through the jejunal vein and approached near the portal vein. The porcine islets were infused with gravity pressure for 8–12 min. After infusion, the vessel was ligated with a 5-0 Prolene suture. After surgery, the tether system was applied for continuous fluid therapy and infusion of low-dose sugar, if necessary.

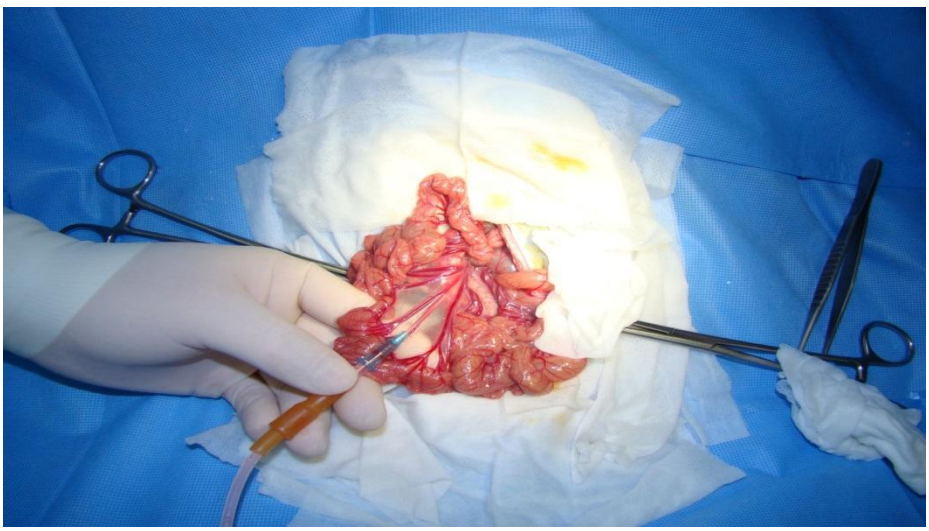

Fig. 2. Porcine islet infusion through the rhesus jejunal vein. A laparotomy was performed followed by exposure of jejunal vein to infuse the islets. A 24- or 22-gauge

catheter was inserted into the jejunal vein and the porcine islets were infused for about 10 min.

5. Immunosuppression

Immunosuppression was induced with anti-human CD154 monoclonal antibody (mAb, 5C8, National Institutes of Health, Bethesda, MD, R051, R080, R082, R084 and R089: Fig. 3.) or with anti-CD40 mAb (2C10R4, NIH NHP Reagent Resource, R086, R088, R091, R095, R092, R087, R008, R131, R143, R147, R144 and R130: Fig.4.) combined with sirolimus (Rapamune®, Pfizer, New York, NY) and rabbit anti-thymocyte globulin (rATG, Thymoglobulin1, Genzyme, Cambridge, MA). Anti-CD154 mAb (20 mg/kg) was intravenously infused on days --10, -7, -4, 0, 3, 7, and 12 of the transplant, weekly for 3 months and then biweekly thereafter. Anti-CD40 mAb (30~50 mg/kg) was intravenously infused on days -4, 0, 4, 7, 10, 14 of the transplant, weekly for three months and then biweekly thereafter. Trough level of sirolimus was 3–8 ng/mL. rATG was administered on days -3, -1 or days -6, -4, -1 or days -6, -4, -1, 0 when insufficient T cell depletions were noticed. Cobra venom factor (CVF) (100 U/kg, Quidel) was administered on day -1 of the transplant to prevent complement activation. TNF-α neutralizing mAb, adalimumab (Humira®, Abbott Laboratories Ltd., Queenborough, UK) was administered subcutaneously 2–3 h before islet infusion with dose of 5 mg/kg of the recipient monkeys. Tacrolimus (Advagraf®, Astellas Pharma Korea, Korea, R092, R087, R008 and R131) was administered daily from day -3 to 30 to achieve stable trough levels (3~6 ng/mL). Tocilizumab (10 mg/kg, Actemra®, Joongwae pharma, Korea, R143, R147, R144 and R130) was infused for 1 hour before islet infusion.

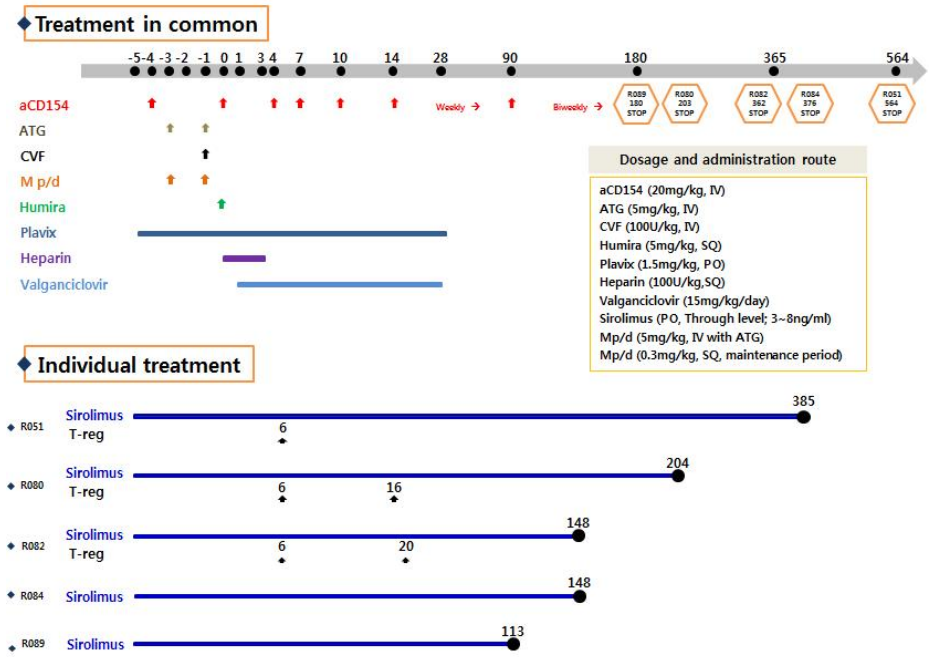

Fig. 3. Anti-CD154 based immune suppression protocols. Anti-human CD154 monoclonal antibody (5C8) was used in R051, R080, R082, R084 and R089 combined with sirolimus and rATG. Anti-CD154 mAb (20 mg/kg) was intravenously infused on days --10, -7, -4, 0, 3, 7, and 12 of the transplant, weekly for three months and then biweekly thereafter. Trough levels of sirolimus were 3–8 ng/mL. rATG was administered on days -3, -1 or days -6, -4, -1 or days -6, -4, -1, 0 when insufficient T cell depletions were noticed. Cobra venom factor (CVF) (100 U/kg, Quidel) was administered on day -1 of the transplant to prevent complement activation. TNF-a neutralizing mAb, adalimumab (Humira®) was administered subcutaneously 2–3 h before islet infusion with a dose of 5 mg/kg of the recipient monkeys. In some monkeys, in vitro expanded autologous regulatory T cells were also added.

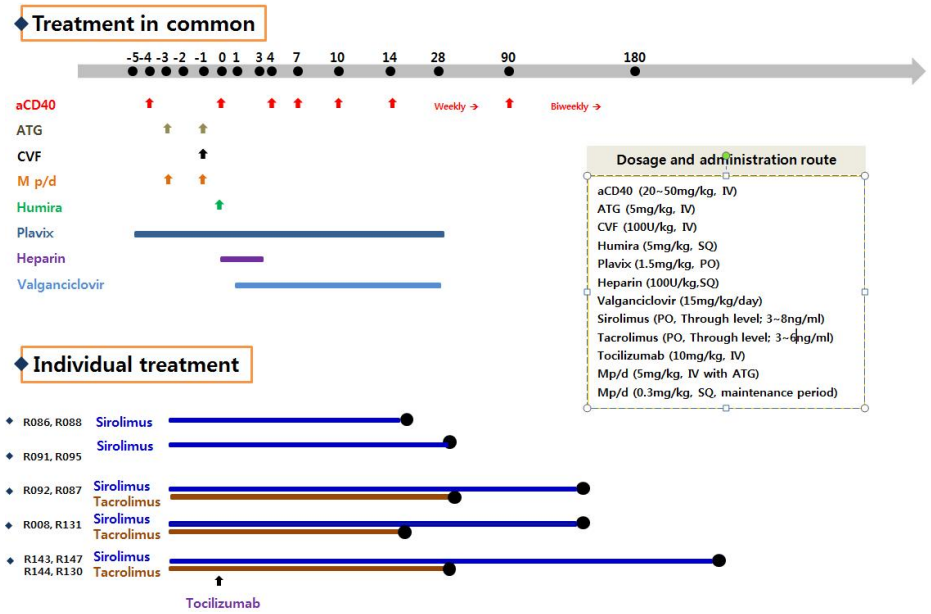

Fig. 4. Anti-CD40 based immune suppression protocols. Anti-CD40 mAb (2C10R4) was used in R086, R088, R091, R095, R092, R087, R008, R131, R143, R147, R144 and R130 combined with sirolimus and rATG. Anti-CD40 mAb (30~50 mg/kg) was intravenously infused on days -4, 0, 4, 7, 10, 14 of the transplant, weekly for three months and then biweekly thereafter. Trough level of sirolimus was 3–8 ng/mL. rATG was administered on days -3, -1 or days -6, -4, -1 or days -6, -4, -1, 0 when insufficient T cell depletions were noticed. Cobra venom factor (CVF, 100 U/kg) was administered on day -1 of the transplant to prevent complement activation. TNF-α neutralizing mAb, adalimumab (Humira®) was administered subcutaneously 2–3 h before islet infusion with dose of 5 mg/kg of the recipient monkeys. Tacrolimus (Advagraf®) was administered in R092, R087, R008 and R131daily from the day -3 to 30 to achieve stable trough levels (3~6 ng/mL). Tocilizumab (10 mg/kg, Actemra®) was infused in R143, R147, R144 and R130 for one hour before islet infusion.

6. Graft outcomes

Graft survival days of each transplanted monkeys were summarized as table.1. Graft survival day was defined as > 0.15 ng/mL porcine C-peptide in the serum as measured by Enzyme-linked immunosorbent assay (ELISA).

Group	CD154					CD40			
Monkey ID	R051	R080	R082	R084	R089	R086	R088	R091	R095
Survival day	>603	180	513	503	180	20	20	41	13
Group	Tacrolimus					Tocilizumab			
Monkey ID	R092	R087	R008	R131		R143	R147	R144	R130
Survival day	60	39	>92	>50		>149	>85	22	11

Table 1. Graft outcomes of each monkey. In CD154 group, graft survival day of each monkey was >603, 180, 513, 503 and 180 days respectively. In CD40 group, graft survival day of each monkey was 20, 20, 41 and 13 days. In Tacrolimus group, graft functions were maintained for 60, 39, >92 and >50 days. In tocilizumab group, graft survivals were >149, >85, 22 and 11 days respectively.

PART 1

$CD4^+/CD8^+$ T cell ratio as a predictive marker for early graft failure in pig to non-human primate islet xenotransplantation with immunosuppression

INTRODUCTION

Recent splendid achievements in the pre-clinical study of pig-to NHP islet xenotransplantation[24] enable us to prepare for clinical trials. Except for islet encapsulation strategies[26], use of immunosuppressive reagent is inevitable to control the immune response to xeno-antigen in clinical porcine islet xenotransplantation[27]. Among the diverse immune response including cytokine-mediated damage to porcine islet [28], T cell immune responses were thought to be one of the most important barriers to be overcome[27,29]. To control the T cell immune response to the xenografts, anti-thymocyte globulin has been broadly used as an induction immunosuppressant in pre-clinical porcine islet xenotransplantation[24,30,31]. As a maintenance immunosuppressant, anti-CD154 based immunosuppression was widely used in various groups[24,29,30,32-35]. However, fatal thromboembolic complications in clinical trials[36] repelled the use of the anti-CD154 antibody in clinics. In this sense, I executed pig islet xenotransplantation in NHP with anti-CD40 and rapamycin sometimes with tacrolimus and tocilizumab. These efforts to establish the clinically applicable immunosuppressive regimens were followed by comprehensive monitoring peripheral blood T lymphocytes because I expected intensive monitoring of peripheral blood T cell subsets could predict graft fate and result in early intervention of immunological harm process. Hence, I comprehensively report the changes of numbers of peripheral blood lymphocyte subsets along with days after porcine islet xenotransplantation in NHPs with various combinations of immunosuppression to find out putative markers to predict the graft fates.

MATERIALS AND METHODS

1. Monkey Grouping

Monkeys were divided into 4 groups depending on the use of different immunosuppressant; CD154 (anti-CD154), CD40 (anti-CD40 alone), tacrolimus (anti-CD40 plus tacrolimus), or tocilizumab group (anti-CD40 plus tacrolimus with tocilizumab). All monkeys were commonly administered with rATG, cobra venom factor (CVF), humira, and sirolimus.

2. Flow cytometry, antibodies and monitoring period.

Flow cytometric analysis of cell suspensions was performed using the following mAbs: FITC-anti-monkey CD3 mAb (FN-18, U-CyTech biosciences, Utrecht, The Netherlands), APC-Cy7-anti-human CD4 mAb (OKT4, BioLegend, San Diego, CA), PE-Cy7-anti-human CD8 mAbs (SK1, eBioscience, San Diego, CA), PE-anti-human CD95 (DX2, eBioscience), PerCP-Cy5.5-anti-human CD28 mAbs (CD28.2, eBioscience). A FACSCantoII flow cytometer (BD, Franklin Lakes, NJ) was used for flow cytometry and data were analyzed using FlowJo software. I monitored subsets of lymphocytes in peripheral blood mononuclear cells (PBMCs) once or twice per weeks until definite graft failure or euthanatize for animal welfare. I included data just before rATG treatments until day post transplantation (DPT) 30-37 for analysis.

3. Statistical analysis

Student's *t*-test with two-tailed was carried out to calculate the *P* values using the statistical software GRAPHPAD PRISM5 (GraphPad Software, Inc., La Jolla, CA). Data are presented as mean ± SD from monkey blood samples unless otherwise stated.

P values less than 0.05 were considered to be statistically significant.

RESULTS

Depletion of T lymphocytes with rATG and time-series kinetics of $CD3^+$ T cell count.

In our experiments, the number of $CD3^+$ T cell after rATG treatment was aiming for less than 500 cells/μL in peripheral blood according to a previous report[30]. Two to five times of rATG administration (5 mg/kg, intravenously) successfully allowed for achieving the $CD3^+$ T cell number of < 500 cells/μL except one monkey (R086) at the DPT 0. $CD3^+$ T cell depletion was also evident in secondary lymphoid organs (Fig. 5). Interestingly, MFI (mean fluorescent intensity) of CD3 immediately after the depletion was significantly lower than that before the depletion (Fig. 6). Recovery kinetics of $CD3^+$ T cell numbers in peripheral blood varied among the monkeys. Four out of seventeen monkeys failed to reach > 1,000/μL during the follow-up period (R092, R131, R147 and R130). It took 38.2±47.7 days (Fig. 7A-E) to reach the 1,000 cells/μL. To evaluate the effect of immunosuppression regimen on T cell repopulation patterns, I divided monkeys into 4 groups and analyzed. However, there were no differences in recovery times between each group (Fig.8).

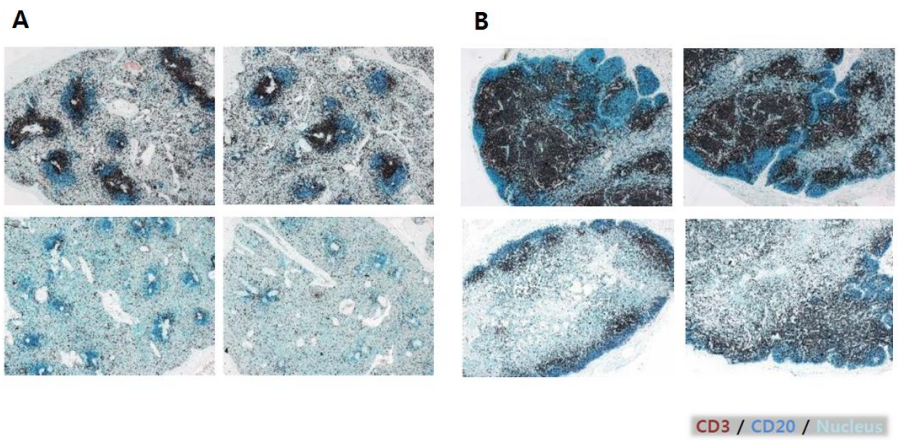

Fig. 5. Secondary lymphoid organs before and after the rATG treatment. (A) Lymphocytes of the spleens (A) and lymph nodes (B) were visualized with brown (CD3) or blue (CD20) color by immunohistochemical staining.

Interestingly, CD3 mean fluorescence index immediate after the depletion were significantly lower than before the depletion (Fig. 1 and 2).

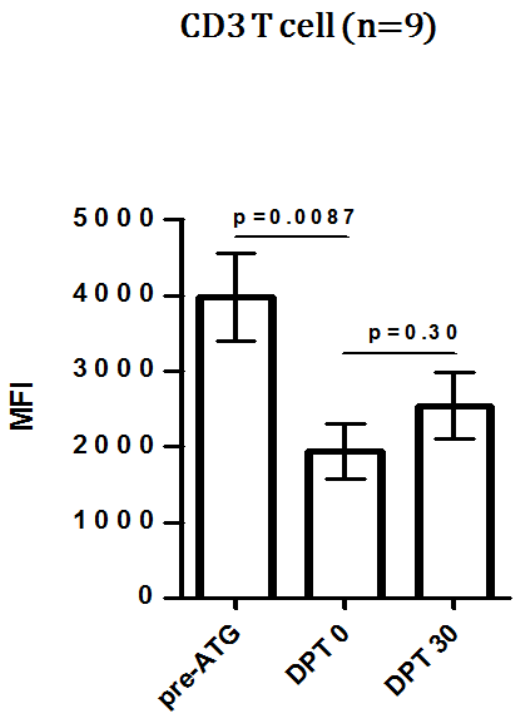

Fig.6. Mean fluorescence intensity of CD3. Mean fluorescence intensity (MFI) of CD3 was measured before the rATG (pre-ATG) treatment, one day after the final treatment of rATG (DPT 0) and thirty days after the transplantation (DPT30). MFI of CD3 molecules was significantly decreased immediately after the depletion. *P*-values were calculated by the two-tailed Student's *t*-test.

Recovery kinetics of $CD3^+$T cell numbers according to the time in peripheral blood was varied. Four monkeys failed to reach > 1000/μL during the follow up period (R092, R131, R147 and R130). It took 38.2 ± 47.7 days (Fig. 7) to reach the number more than 1000 cells /μL on average of 13 monkeys. There are no differences of recovery times between each group (Fig.8).

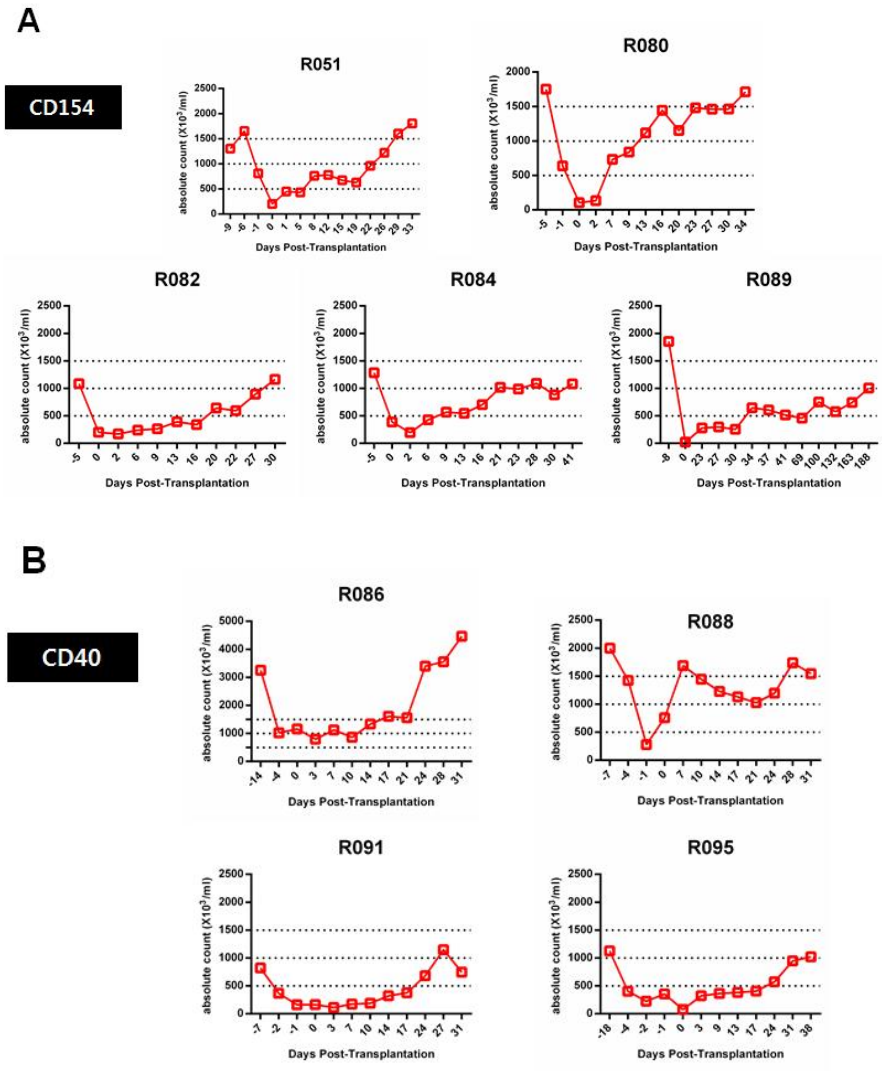

C

Tacrolimus

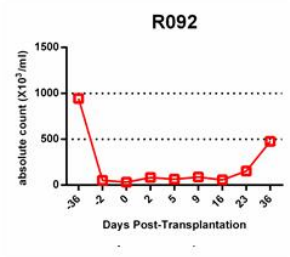

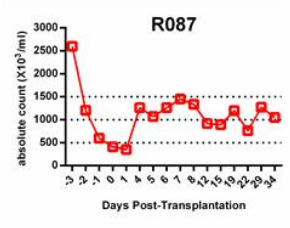

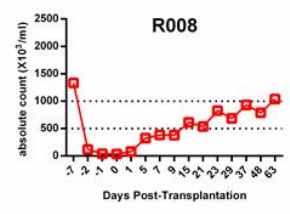

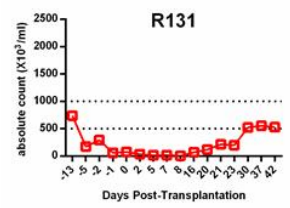

D

Tocilizumab

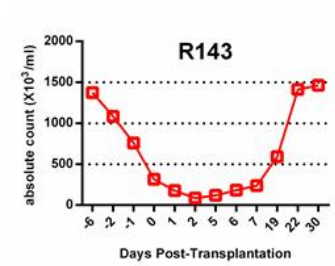

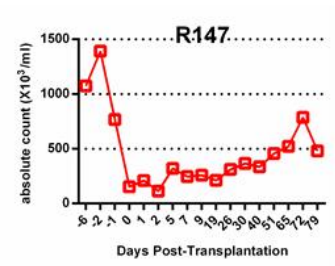

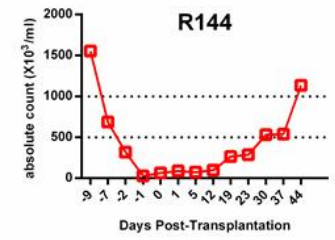

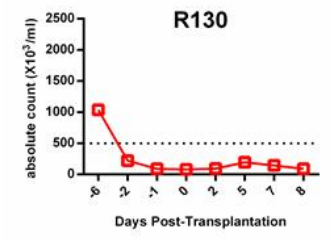

E

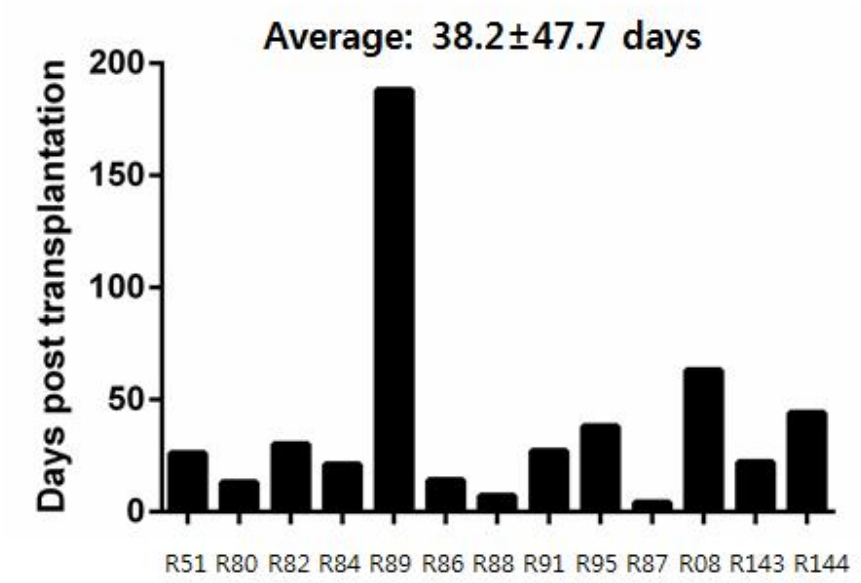

Fig. 7. Time-series $CD3^+$ T cell numbers after rATG treatment and recovery times of $CD3^+$T cell numbers. Data were displayed before the rATG treatment till DPT 30 and $CD3^+$T cell counts reached more than 1000 cells/μL. (A) CD154 group. (B) CD40 group. (C) Tacrolimus group. (D) Tocilizumab group. (E) First days when $CD3^+$T cell was count more than 1000 cells/μL.

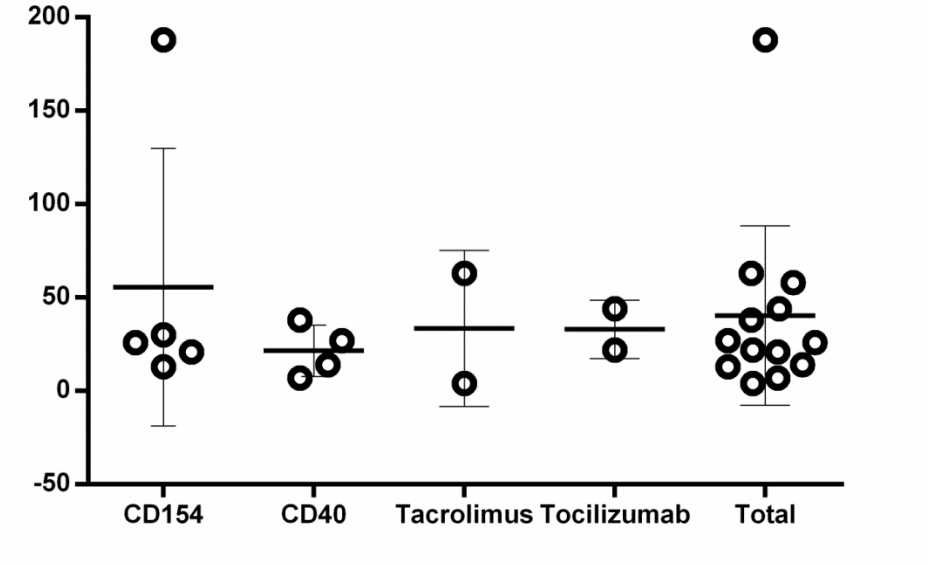

Fig. 8. T cell recovery days in each group. T cell recovery times of thirteen monkeys were displayed according to the different immunosuppression protocols except for four monkeys (R092, R131, R147 and R130). There are no differences of recovery times between each group.

Homeostatic repopulation of $CD4^+$ and $CD8^+$ T cells with various combinations of immunosuppression.

Before the depletion of $CD3^+$ T cells, almost of the monkeys showed that their $CD4^+$ T cell count was more than or tantamount to $CD8^+$ T cell count except for two monkeys (R086, R088). However, after the rATG treatment, 14 out of 17 monkeys exhibited $CD8^+$ T cell count dominance over $CD4^+$ T cell count (Fig. 9A-F). These results suggested that after the depletion of T cells, homeostatic repopulation of $CD8^+$ T cells happened more vigorously than that of $CD4^+$ T cells.

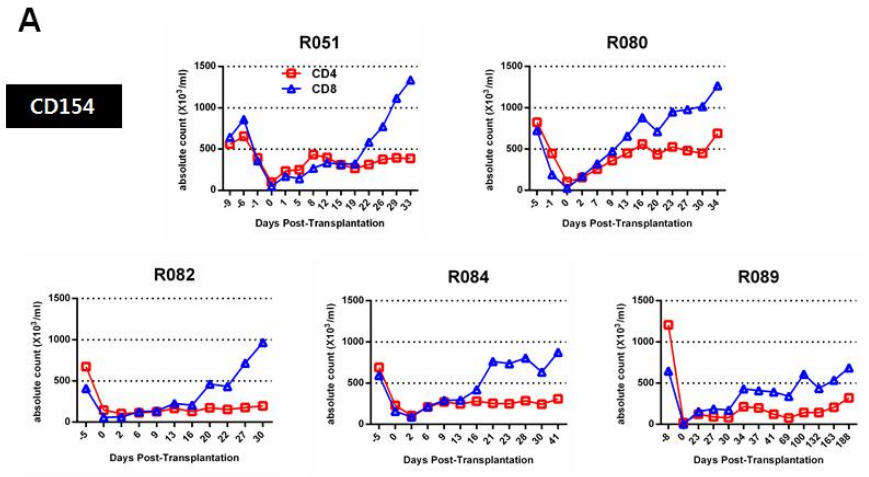
A
CD154
R051
CD4
CD8
absolute count (X10³/ml)
Days Post-Transplantation
R080
R082
R084
R089
B
CD40
R086
R088
R091
R095

C

Tacrolimus

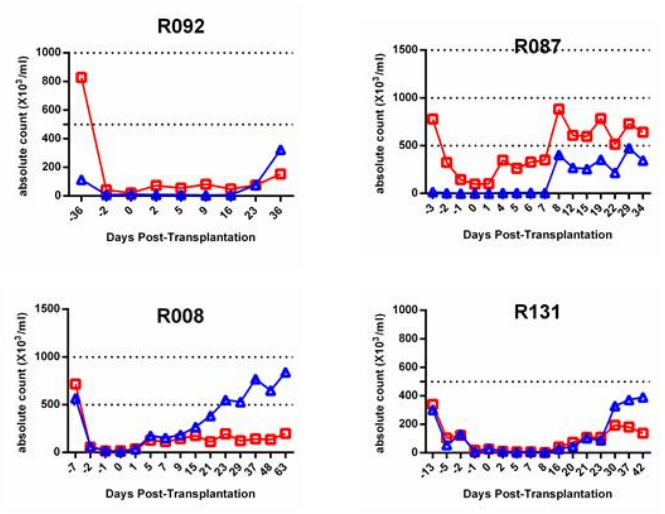

D

Tocilizumab

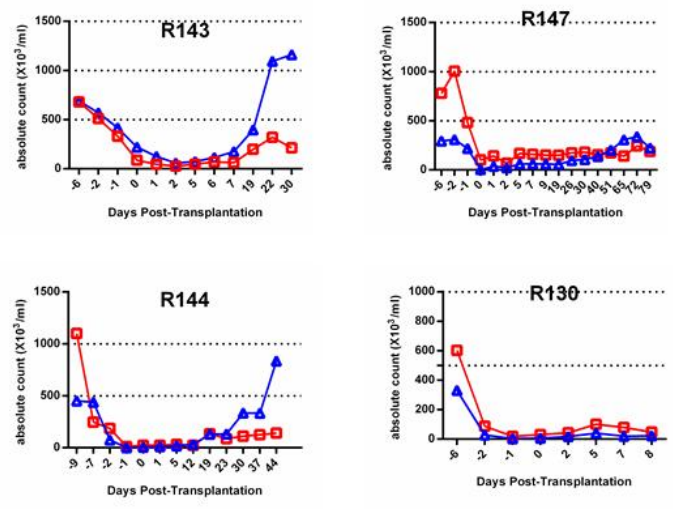

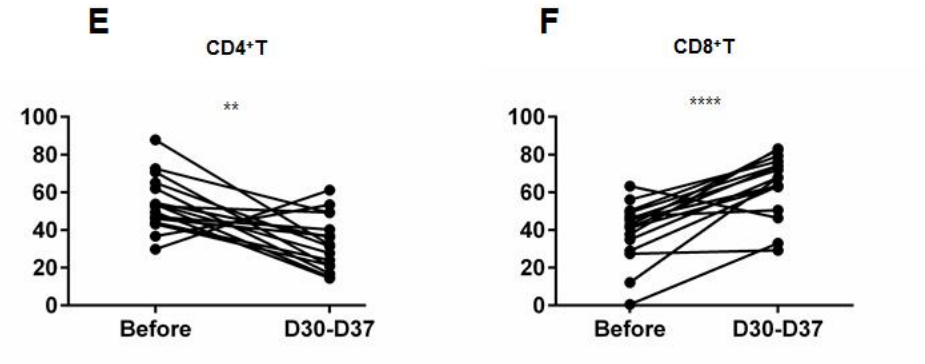

Fig.9. Time-series $CD4^+$ T cell and $CD8^+$ T cell numbers after rATG treatment. (A) CD154 group. (B) CD40 group. (C) Tacrolimus group. (D) Tocilizumab group. (E) $CD4^+$ T cells percentage from total $CD3^+$ T cells before and after the rATG treatment. (F) $CD8^+$ T cell percentage from total $CD3^+$ T cells before and after the ATG treatment. **: $p < 0.01$ and ****: $p < 0.0001$ by the two-tailed Student's *t*-test.

Major populations of repopulated $CD8^+$T cell

Next, I sought to examine which functional $CD8^+$ T cell subset was primarily repopulated. Rhesus monkey T cells could be classified as three functional T cell subsets such as naïve T cells ($CD28^+/CD95^-$), central memory T cells ($CD28^+/ CD95^+$) and effector memory T cells ($CD28^-/CD95^+$) [37,38]. Hence, I classified $CD8^+$ T cells in peripheral blood of the monkeys with these surface markers. As shown in Fig. 10A-D, the majority of repopulated $CD8^+$ T cells belonged to an effector memory phenotype.

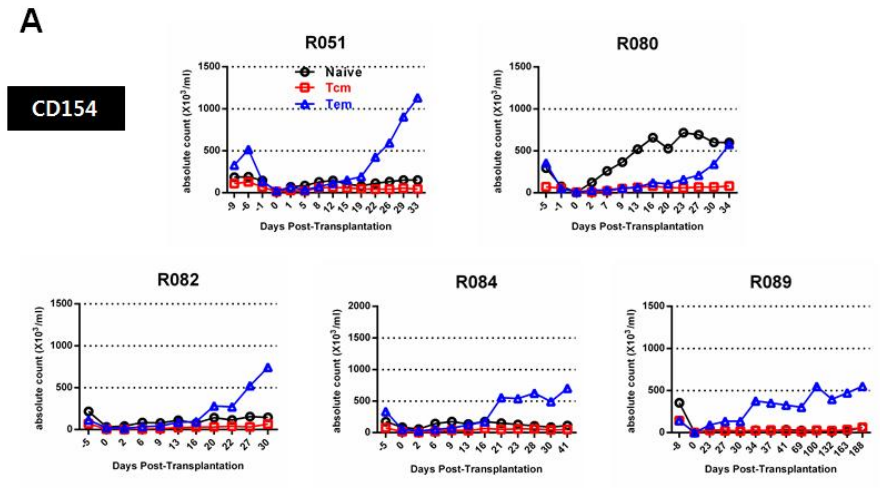
A
CD154
R051
Naive
Tcm
Tem
R080
R082
R084
R089
absolute count (X10³/ml)
Days Post-Transplantation

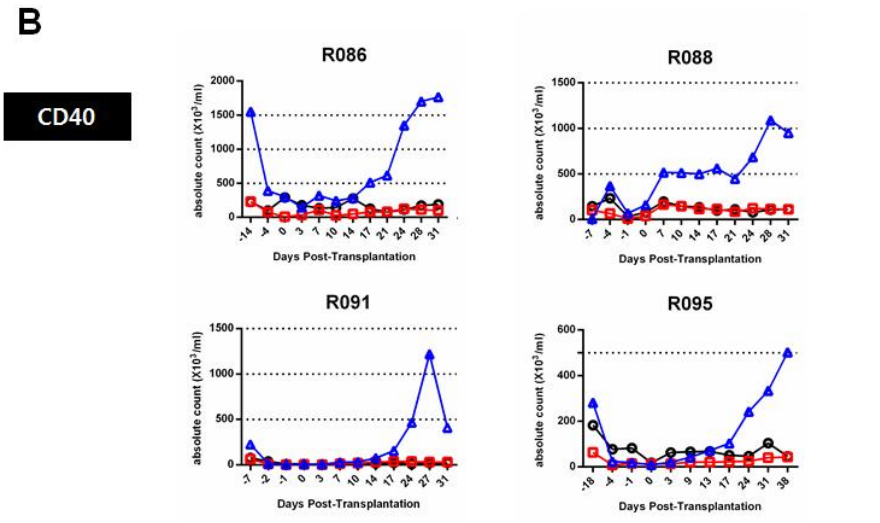
B
CD40
R086
R088
R091
R095
absolute count (X10³/ml)
Days Post-Transplantation

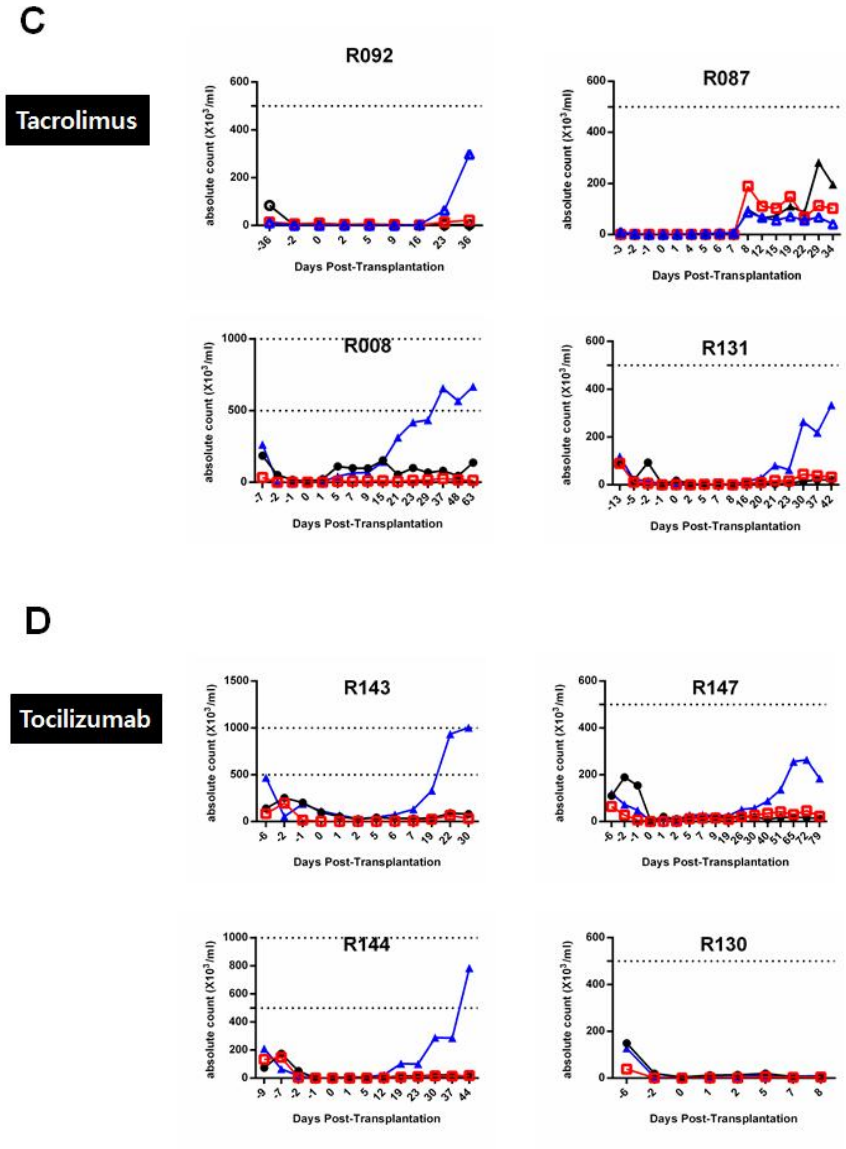

Fig. 10. Time-series functional subpopulations of $CD8^+$ T cell numbers after rATG treatment. (A) CD154 group. (B) CD40 group. (C) Tacrolimus group. (D) Tocilizumab group. Naïve, central memory cells, and effector memory cells represent $CD95^-CD28+$, $CD95^+CD28^+$, and $CD95^+CD28^-CD8^+$ T cells, respectively.

Correlation of T cell subtype monitoring results with early graft survival.

It is easily speculated that recovery of T cell populations in peripheral blood indefinitely increases the risk of rejection. Hence, I wanted to find out the responsible T cell populations which had relations with the early graft rejection or putative surrogate markers that could predict early graft failure. However, single functional T cell subpopulations which have consistent positive correlations with graft fate were not evident. Because I was impressed that $CD4^+/CD8^+$ T cell ratio within 30 DPT could be related to graft survival in some monkeys while carrying out our experiments, I examined whether this ratio could be used as a putative surrogate marker to predict early graft failure in our experimental setting. Since four different immunosuppression regimens were used, I compared $CD4^+/CD8^+$ T cell ratio between long-term graft-survived monkeys (LGSM) and short-term graft-survived monkeys (SGSM) in each group. $CD4^+$ and $CD8^+$ T cell counts from 0 DPT to 30 DPT were used for analysis and data showing less than 100 cells/μL of $CD8^+$ T cell were not included. As a result, a significant difference of $CD4^+/CD8^+$ T cell ratio was observed between LGSM and SGSM (Fig. 11). However, there were no discernable differences of ratio in each group between LGSM and SGSM except tacrolimus group (Fig. 12A-D).

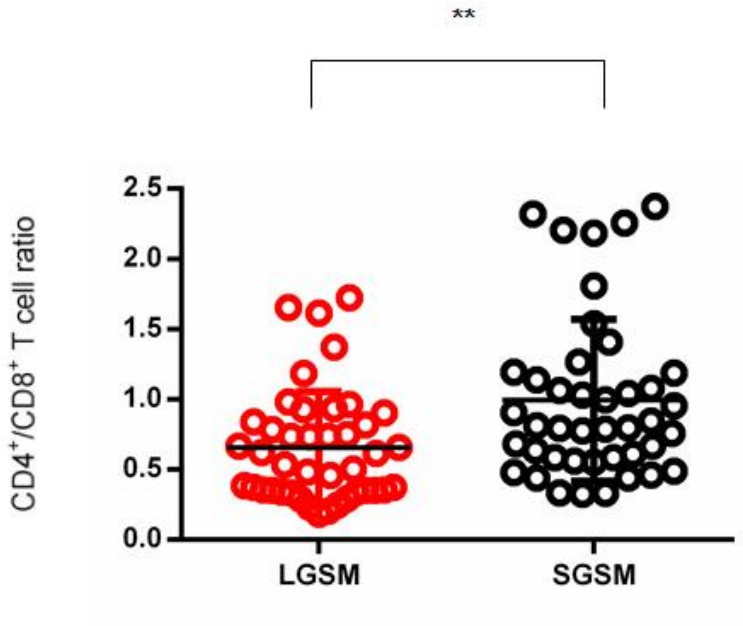

Fig. 11. $CD4^+/CD8^+$ T cell ratio of SGSM and LGSM in each group.. $CD4^+/CD8^+$ T cell ratio was significantly lower in LSGM than SGSM. SGSM: Short-term graft survival monkey, LGSM: Long-term graft survival monkey. Each dot represents $CD4^+/CD8^+$ T cell ratio of single time point from DPT 0 to DPT 30. **: $p < 0.01$ by the two-tailed Student's *t*-test.

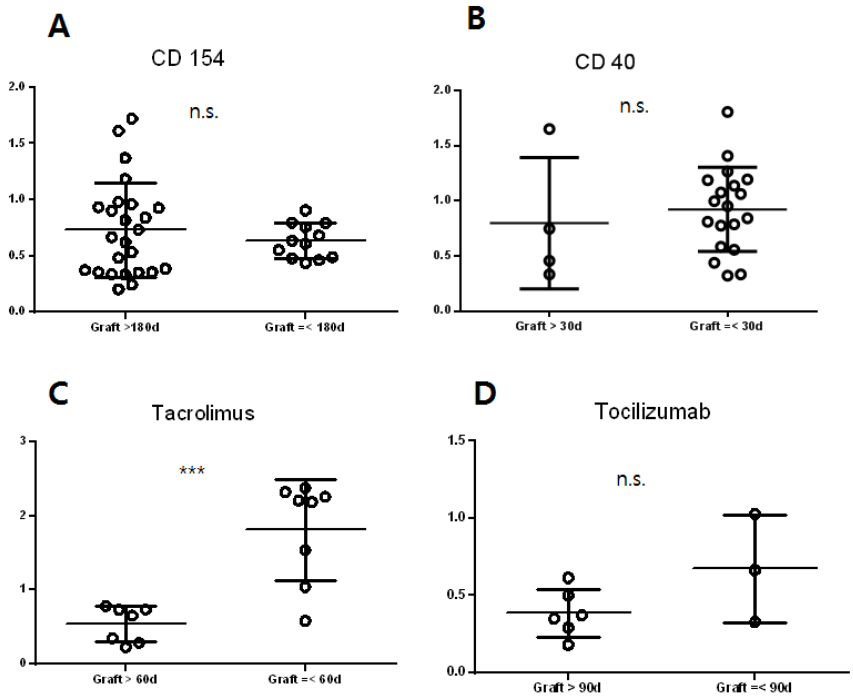

Fig. 12. $CD4^+/CD8^+$ T cell ratio in each group. Except for tacrolimus group, there were no differences between LGSM and SGSM. The criterion of graft survival day which divided monkeys into LGSM and SGSM was passing 180 DPT in CD154 group, 30 DPT in CD40 group, 60 DPT in tacrolimus group, and 90 DPT in tocilizumab group, respectively, without rejection. *n.s*; not significant. ***: $p < 0.001$ by the two-tailed Student's *t*-test.

DISCUSSION

Monitoring status of cell-mediated immunity in patients after organ transplantation is very important. On one hand, excessive immunosuppression renders the patients vulnerable to numerous infectious sources. On the other hand, insufficient use of immunosuppressant results in graft rejection by T cells. However, valuable parameters of cellular immune monitoring post-organ transplantation are still lacking[39]. Enzyme-linked immunosorbent assay was attempted to monitor the porcine antigen-specific T cell immune responses after porcine islet transplantation in NHPs[29,34,40]. Unfortunately, it could not be entirely validated despite labor intensive method. Our extensive T cell immune monitoring consists of enumerating $CD4^+$, $CD8^+$ T cells and further classifying differential functional T cell subsets such as $CD4^+CD95^+CD28^+$ central memory cells and $CD4^+CD95^+CD28^-$ effector memory cells enabled us to study the time-series kinetics of T lymphocyte subsets. I demonstrated that after the depletion of T cells, it took about one month to reach the lower limit of ordinary $CD3^+$ T cells number (1000 cells/μL)[41] in the peripheral blood of rhesus monkey (Fig. 7E). Lower values of mean fluorescent intensity (MFI) of CD3 molecules immediately after the depletion than that before the depletion were observed. It could be explained by two possibilities: First, CD3 populations with lower MFI could have been more resistant to rATG treatment. Second, epitopes of CD3 molecules to which fluorescence activated cell sorting (FACS) antibody have to access were masked by polyclonal rATG-binding. Considering the restoration of MFI at 30 DPT, the latter explanation seems more feasible.

After rATG treatments, $CD3^+$ T cell counts were reduced to < 500 cells /μL except

R086 (Fig. 7A-D). After then, $CD8^+$ T cells started to increase more rapidly than $CD4^+$ T cells. As I confirmed that our rATG protocol depleted T cells in not only peripheral blood but secondary lymphoid organ including lymph nodes and spleen (Fig. 5), rapid $CD8^+$ T cell expansion is probably due to the tendency of $CD8^+$ T cell's quicker proliferation than $CD4^+$ T cells in lymphopenic environment[42,43]. Furthermore, I noticed that the major populations of expanded $CD8^+$ T cells were $CD95^+CD28^-$ effector memory cells (Fig. 10A-D). This observation was concordant with previous reports in solid organ transplantation in humans[44,45].

I eventually showed that $CD4^+/CD8^+$ ratio within 30 DPT had correlations with relatively early graft failure. It is not clear that $CD4^+/CD8^+$ ratio was the cause or result of the graft survival. However, our group previously suggested that graft protective roles of $CD8^+CD28^-$ cells in islet xenotransplantation[24]. The rapid expansion of these graft protective $CD8^+CD28^-$ cell populations after the rATG mediated T lymphocyte depletion might have influenced the better survival of grafts. Even though there have been several reports which claimed the regulatory functions of $CD8^+CD28^-$ cells in various conditions[46-48], there were few studies that dealt with this population of cells after homeostatic expansion condition following lymphodepletion.

In conclusion, I for the first time, report the T cell functional subset's time-series kinetics after rATG treatment in NHP after porcine islet xenotransplantation. As a result, I suggest $CD4^+/CD8^+$ T cell ratio as the putative marker for an early graft failure.

PART 2

Porcine antigen-specific IFN-γ ELISpot as a potentially valuable tool for monitoring cellular immune responses in pig to non-human primate islet xenotransplantation.

INTRODUCTION

Islet transplantation has potential as a highly effective treatment for type 1 diabetes patients suffering from severe hypoglycemia[49]; however, a shortage of human donor islets makes it hard to routinely apply this approach in clinical practice. Therefore, porcine islet xenotransplantation has been proposed as one of the best alternatives. In fact, recent reports in pre-clinical trials suggested the prospect of this approach[24,50]. These results, together with the implementation of guidelines for porcine islet clinical trials by the International Xenotransplantation Association (IXA)[51], imply the clinical application of porcine islet xenotransplantation may be imminent. Following porcine islet xenotransplantation, there is a need for close monitoring of cellular immune responses to donor porcine antigens in order to diagnose cellular rejection over the course of the follow-up period. In this context, the ELISpot assay has been widely used to monitor cellular immune responses in humans. For example, following human kidney transplantation, the ELISpot assay has proved useful for screening of patients at high risk for acute[52-55] or chronic[56] graft rejection. Also, an increased number of IFN-γ-producing donor–reactive memory cells was detected by ELISpot assay in patients who did experience an acute rejection[57]. Recently, Standardization and cross-validation of allo-reactive IFN-γ ELISpot assay were reported in clinical allo-transplantation[58,59]. However, the utility and comprehensiveness of the ELISpot assay are yet to be determined for pig-to-NHP islet xenotransplantation. Moreover, use of ELISpot analyses on serial peripheral blood samples collected after transplantation has not been previously reported. Therefore, in this study, first, I determined optimal conditions for the ELISpot assay. Second, the retrospective IFN-γ ELISpot assay was conducted

using a time-series of PBMC samples from the monkeys with prolonged porcine islet grafts. Finally, the utility of the ELISpot assay as a tool for monitoring porcine antigen-specific cellular immune responses was assessed by comparing the number of IFN-γ spots with histopathological examination of biopsied liver samples.

MATERIALS AND METHODS

1. Animals

Four rhesus monkeys were used in this study (R080, R082, R084, R089).

2. PBMC and spleen cell isolation

Blood samples were obtained from the rhesus monkeys that were recipients of porcine islet transplantation. PBMCs were isolated from heparinized blood by density gradient centrifugation using Ficoll-paque™ PLUS (GE Healthcare, Uppsala, Sweden). Whole blood was diluted 1:1 with sterile PBS, aliquoted into 50-mL centrifuge tubes and then one volume of Ficoll was under layered using a sterile pipette to dilute the blood volume (1:2). The suspension was centrifuged at 2100 r.p.m. (950 ×g) in a swinging bucket rotor in a table-top centrifuge for 30 min at room temperature with no brake. PBMCs were isolated from the interface, washed in RPMI 1640 media containing 10% FBS and the cell pellet was re-suspended in 50 mL of sterile PBS and re-centrifuged at 200 × g for 10 min at room temperature in order to remove platelets. Cells were counted using a hemocytometer. Splenic single cell suspensions in 10% FBS RPMI media were produced by mechanical disruption of the tissue using the flat end of a sterile 30 cc syringe plunger to pass the disrupted tissue through a cell strainer (no. 70 mesh size, SPL, Kyeonggi-do, Korea). Mononuclear cells were then isolated from this cell suspension by density gradient centrifugation using Ficoll-paque™ PLUS, as outlined above.

3. Cryopreservation

Cells were pelleted (300 × g) by centrifuge for 5 min in a swinging bucket rotor in 15-mL tubes and were then re-suspended in freezing solution comprised of 90% FBS and 10% DMSO (Sigma, St. Louis, MO) at room temperature. The cells were placed in a freezer box at -80℃ for 24–48 h and were then transferred into liquid nitrogen.

4. Cell sorting and gating strategy for ELISpot assay

PBMCs were stained with FITC-anti-human CD2 (RPA-2, eBioscience), APC-anti-human CD16 (3G8, BD Pharmingen), APC-Cy7-anti-human CD4 mAb (OKT4, BioLegend) and were then sorted using a FACSAria II (BD Immunocytometry Systems, San Jose, CA). $CD2^{+}CD16^{-}$ cells were considered as T cell and used for determining an optimal number of responder cell, $CD2^{+}CD16^{-}CD4^{+}$ cells were considered as $CD4^{+}$ T cell, $CD2^{+}CD16^{-}CD4^{-}$ cells were considered as $CD8^{+}$ T cell.

5. Porcine islet single cell preparation for third party islet stimulated ELISpot assay

Third party islets were obtained from our porcine islet storage system. Porcine islets from SNU mini-pig or farm pig were routinely isolated and stored with isolation record. To acquire single cells of porcine islet cluster, which would be used for stimulator cells in ELISpot assay, porcine islets were treated with 0.1× trypsin (TrypLE™ Express, Gibco by Life Technology), and then incubated for 3 mins, at 37℃ in a water bath.

6. IFN-γ ELISpot assay.

The frequency of IFN-γ–secreting, pig antigen-specific T cells in the peripheral blood of monkeys was measured using an ELISpot kit (Mabtech, Nacka Strand, Sweden). Briefly, PVDF-plates (EMD Millipore Corporation, Billerica, MA) were treated with 50μL of 70% ethanol per well for 2 min. The plates were washed three times with sterile water (100μL/well). IFN-γ capture antibody was diluted to 15μg/mL in sterile PBS, pH 7.4, and then added and incubated overnight at 4℃. IFN-γ capture antibody-coated plates were washed four times with sterile PBS (100μL/well) and blocked for 60 min with 10% FBS–supplemented RPMI 1640 media at 37℃ in a 5% CO_2 incubator. For determining optimal responder cell number, each of 2×10^5, 5×10^5, 1×10^6 monkey T cells were cultured with 5×10^5, 1×10^6 porcine PBMCs (30Gy irradiation) respectively. In time-series monitoring of PBMCs using IFN-γ ELISpot assay, 2.5×10^5 monkey PBMCs were cultured with 5×10^5 porcine splenocytes (30Gy irradiation) in RPMI 1640 media supplemented with 10% FBS for 40 h at 37°C in a 5% CO_2 incubator. In the third party, porcine islets donor assay, 5×10^4 islet single cells were used instead of porcine splenocytes as stimulator cells. In some cases, 3μL/mL of anti-CD28 Ab (CD28.2, eBioscience) was added. After a 40-h culture, cells were removed and the plates were washed five times with distilled water (100μL/well). Biotin-conjugated detection antibody (7-B6-1-biotin) diluted at 1:1000 in 100μL PBS containing 0.5% FBS was then added and incubated for 2 h at room temperature. The plates were washed five times with PBS (100μL/ well). Streptavidin-Alkaline phosphatase diluted at 1:1,000 in 100μL PBS containing 0.5% fetal bovine serum was then added and incubated for 1 h at room temperature. The plates were washed five times with PBS, and 100μL BCIP/ NBP substrate was added. Color development was

stopped by washing with tap water. The resulting spots were counted on a computer-assisted ELISpot Reader System (AID, Straßberg, Germany).

7. Flow cytometry and antibodies

Flow cytometric analysis of cell suspensions was performed using the following mAbs: FITC-anti-monkey CD3 mAb (FN-18, U-CyTech biosciences), PE-anti-human CD95 (DX2, eBioscience), PerCP-Cy5.5-anti-human CD28 mAbs (CD28.2, eBioscience), PE-Cy7-anti-human CD8 mAbs (SK1, eBioscience), APC-Cy7-anti-human CD4 mAb (OKT4, BioLegend). A FACSCantoII flow cytometer (BD) was used for flow cytometry and data were analyzed using FlowJo software. For intracellular staining of Foxp3, cells were stained with a commercially available kit (eBioscience). For analysis of Foxp3 expression at the single-cell level, cells were first stained for the expression of the respective surface molecules (FITC-anti-CD4 mAb (OKT4, eBioscience) and, after fixation and permeabilization, were incubated with APC-anti-human Foxp3 mAb (PCH101, eBioscience) or the IgG2a isotype control (eBR2a, eBioscience), respectively, based on the manufacturer`s recommendations.

8. Biopsy and immunohistochemistry

Immunohistochemical staining was conducted as described previously[24]. Briefly, liver biopsy samples from recipient monkeys were fixed in 10% neutral buffered formalin, and embedded in paraffin. Paraffin-embedded tissues were sectioned at 4μm using a microtome. Sections were stained with a primary antibody cocktail for CD3 (DAKO, Carpinteria, CA) and CD68 (Thermo Scientific, Bartlesville, OK). Then, appropriate enzyme-conjugated secondary antibodies and substrates (Thermo Scientific) were

sequentially added for color development. After washing, sections were stained with a primary antibody against insulin (Santa Cruz Biotechnologies, Dallas, TX). Then, secondary antibody and substrate were sequentially added for color development. The stained samples were observed using a Carl Zeiss Axio Imager A1 microscope and images were taken with AxioVision software (Carl Zeiss, Oberkochen, Germany).

9. Statistical analysis

Student's *t*-test with two-tailed was carried out to calculate the *P* values using the statistical software GRAPHPAD PRISM5 (GraphPad Software, Inc.).. Data are presented as mean ± SD from n monkey blood samples, unless otherwise stated. *P* values less than 0.05 were considered to be statistically significant.

RESULTS

1. Set up of IFN-γ ELISpot assay

First, the appropriate number and ratio of responder and stimulator cells for establishing the IFN-γ ELISpot assay were determined using PBMC samples from pre-transplant monkeys. It was found that incubation of 2.5×10^5 responder cells with 5.0×10^5 stimulator cells provided the most consistent and reliable results. When more than 2.5×10^5 responder cells were used, too many spots were produced, making the assay hard to read. Likewise, fewer stimulator cells produced too few spots (Fig. 13). Since stimulation with either porcine PBMCs or splenocytes produced similar results (Fig. 13), I decided to use porcine splenocytes as stimulators for the following experiments. Next, I wanted to clarify whether the provision of a costimulatory signal could increase the sensitivity of the assay. Interestingly, the difference was not observed when anti-CD28 mAb was further provided in the assay (Fig. 13). Finally, I sought to determine which subset of monkey T cells produce IFN-γ in response to porcine splenocytes. After cell sorting (Fig. 14), $CD4^+$ T cells or $CD8^+$ T cells were incubated with pig splenocytes. Although direct evidence is lacking, the data supported that $CD8^+$ T cells were the major IFN-γ producing cells in our assay, although $CD4^+$ T cells could produce a significant number of spots (Fig. 13).

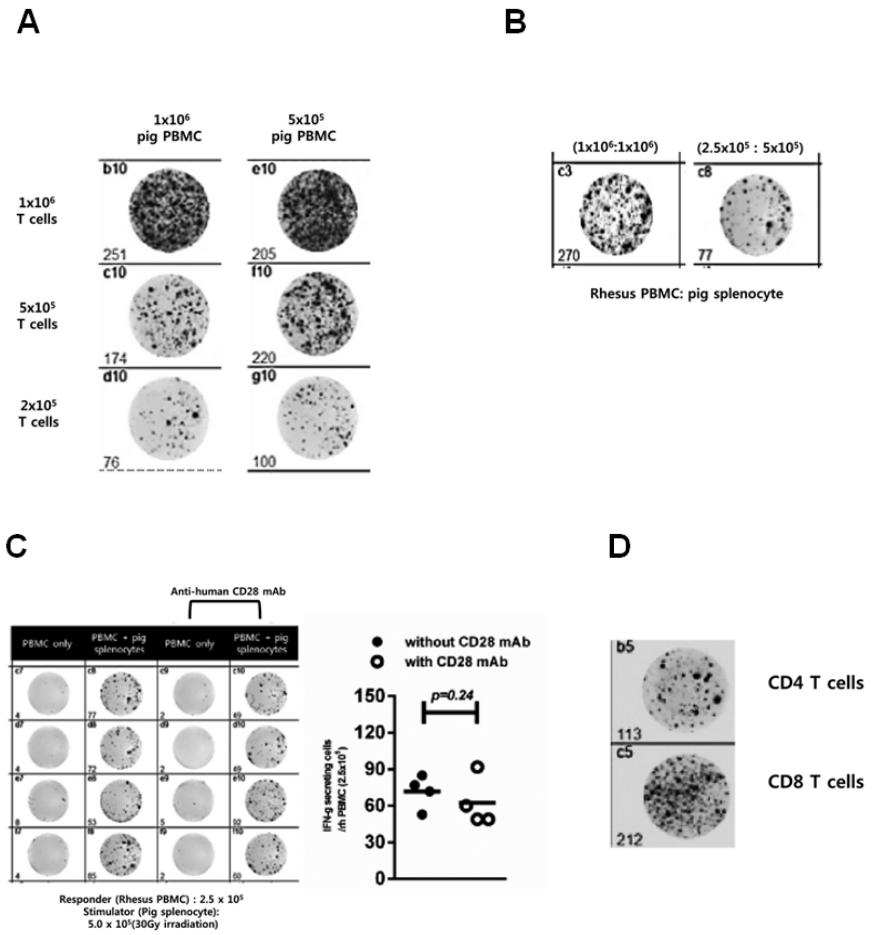

Fig 13. Optimization of experimental conditions for the porcine antigen-specific IFN-γ ELISpot assay.

(A and B) Optimal numbers of monkey T cells and porcine PBMCs or splenocytes were titrated. (C) PBMCs samples from four independent monkeys were treated with anti-CD28 (3μL/mL) antibody followed by porcine antigen-specific IFN-γ ELISpot assay. (D) CD4 or CD8 T cells were sorted from monkey PBMCs and 2.5×10^5 sorted T cells were incubated with porcine splenocytes followed by the ELISpot assay. *P*-value was calculated by the two-tailed Student's *t*-test.

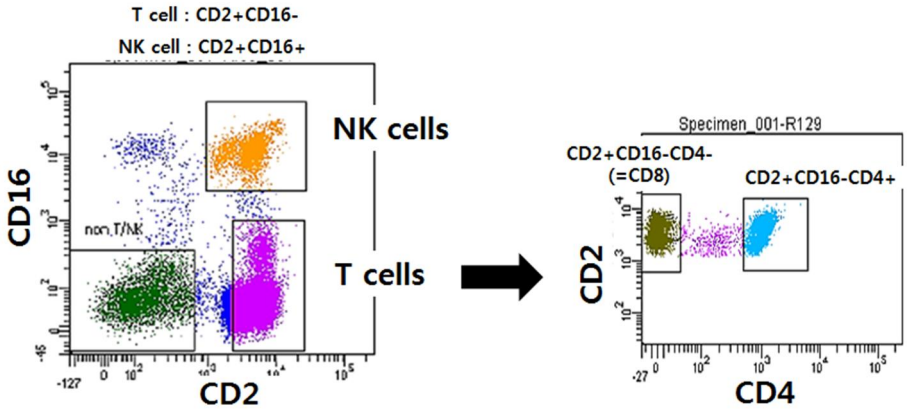

Fig 14. Cell sorting strategy. $CD2^{+}CD16^{-}CD4^{+}$ cells were considered as $CD4^{+}$ T cell $CD2^{+}CD16^{-}CD4^{-}$ cells were considered as $CD8^{+}$ T cells

2. Time-series monitoring of PBMCs using IFN-γ ELISpot assay

Recently, our group reported the consistent long-term survival of islet grafts in five monkeys [24] and these monkeys eventually failed to maintain normoglycemia. PBMC samples from these animals were taken and then stored. Hence, in this study, I was able to perform sequential IFN-γ ELISpot assay using these samples (Fig. 15A-H and 16A-D). I found that all PBMC samples produced an increased number of donor splenocyte-specific IFN-γ spots only after exogenous insulin requirement (Fig. 15A-H), suggesting this assay is not sensitive enough to predict porcine antigen-specific cellular rejection occurring insidiously or gradually.

A

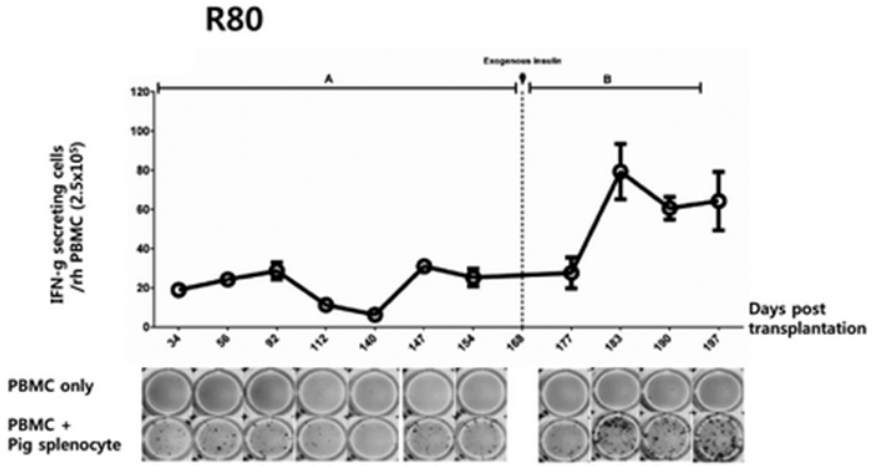
R80
Exogenous insulin
A
B
IFN-g secreting cells /rh PBMC (2.5x10⁵)
120
100
80
60
40
20
0
34
58
92
112
140
147
154
168
177
183
190
197
Days post transplantation
PBMC only
PBMC + Pig splenocyte

B

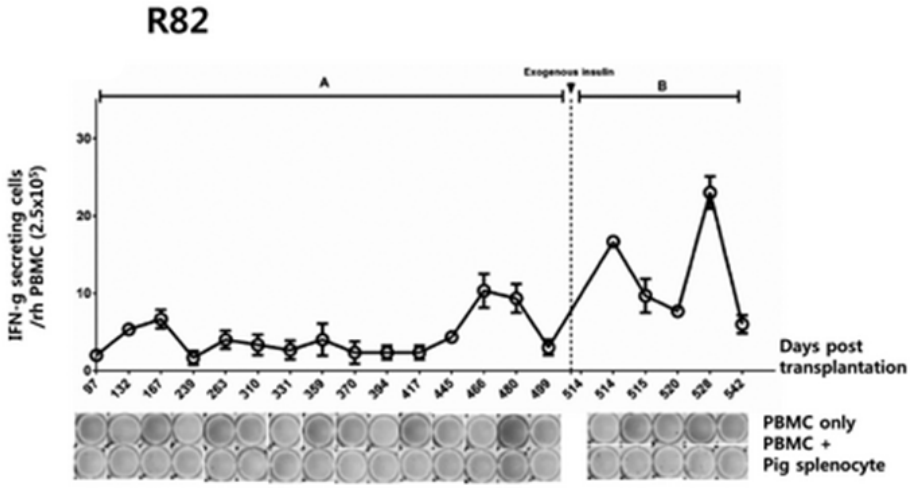
R82
Exogenous insulin
A
B
IFN-g secreting cells /rh PBMC (2.5x10⁵)
30
20
10
0
97
132
167
239
253
310
331
359
370
394
417
445
466
480
499
514
514
515
520
528
542
Days post transplantation
PBMC only
PBMC + Pig splenocyte

C

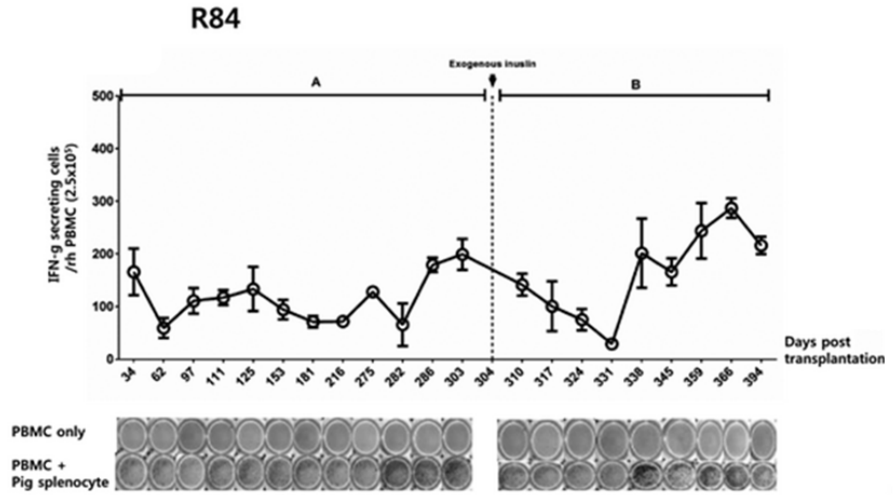
R84
Exogenous insulin
A
B
IFN-g secreting cells /rh PBMC (2.5x10⁵)
500
400
300
200
100
0
34 62 97 111 125 153 181 216 275 282 286 303 304 310 317 324 331 338 345 359 366 394
Days post transplantation
PBMC only
PBMC + Pig splenocyte

D

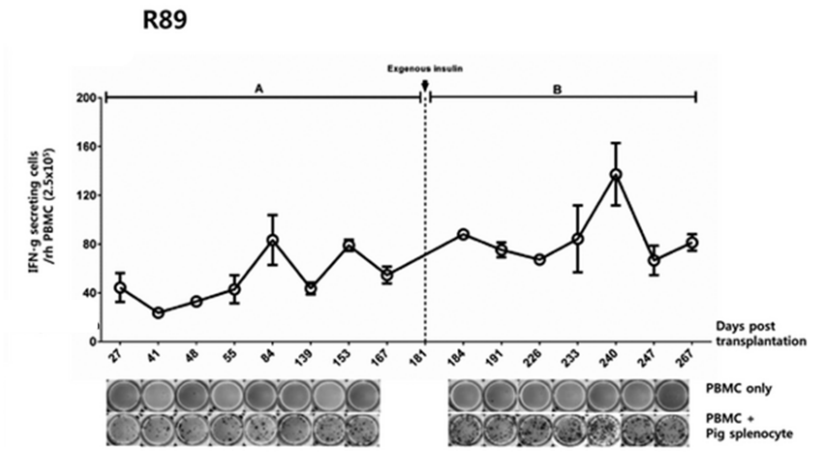
R89
Exgenous insulin
A
B
IFN-g secreting cells /rh PBMC (2.5x10⁵)
200
160
120
80
40
0
27 41 48 55 84 139 153 167 181 184 191 226 233 240 247 267
Days post transplantation
PBMC only
PBMC + Pig splenocyte

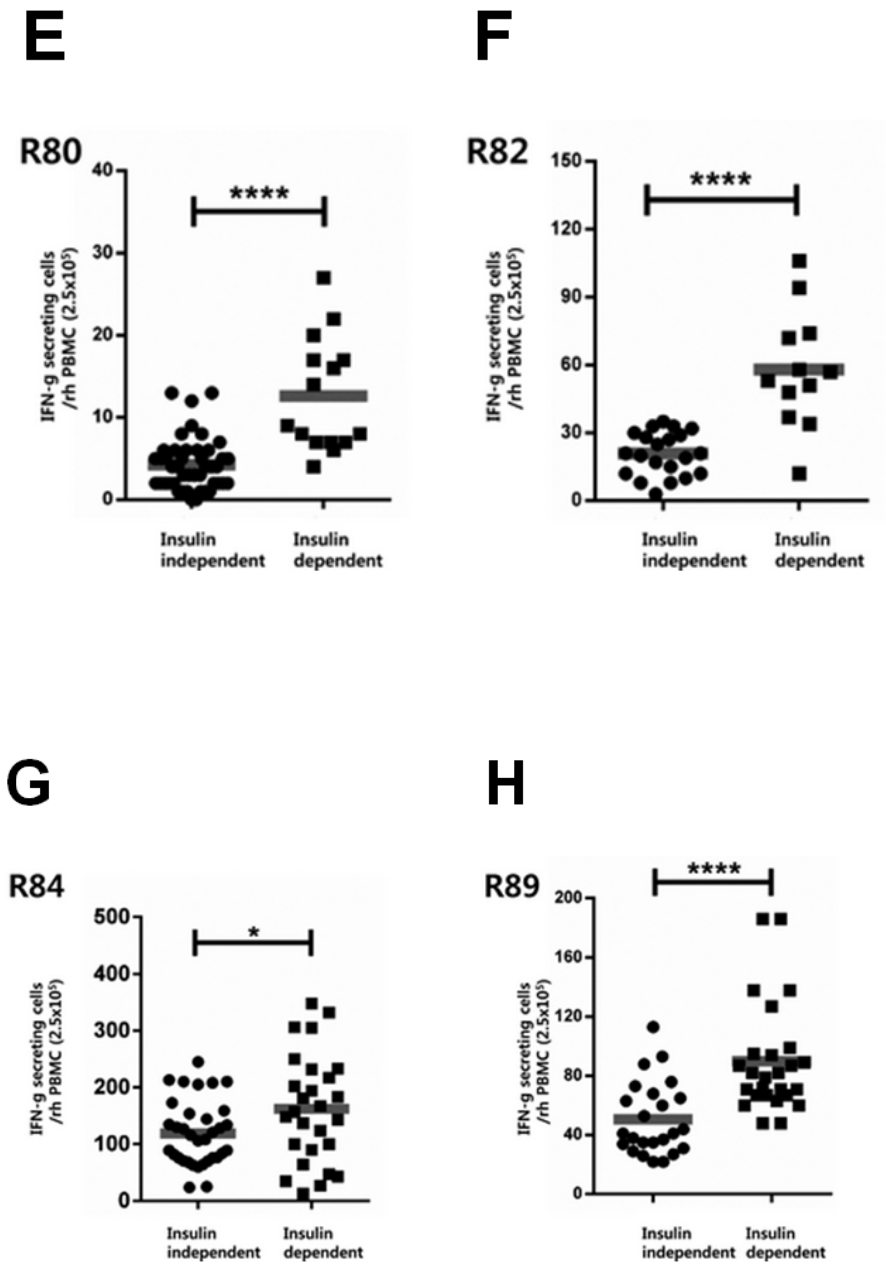

Fig.15. IFN-γ ELISpot performed on a time-series PBMC samples from porcine islet recipient monkeys., The small figures of the first line below the graph are medium only well, second line figures were recipient PBMC with pig splenocytes well. (A-D) After

porcine islet transplantation, PBMCs from recipient monkeys were sampled at different time-points and stored. Stored PBMCs (2.5×10^5) were co-cultured with 5.0×10^5 splenocytes for 40 hours. (E-H) Comparison of spot numbers between the pre- and post-graft rejection period. Rejection day was defined as the first day of two consecutive days of increasing blood glucose level > 200 or exogenous insulin requirement > 0.2 U. Upper-left number of each graph indicates monkey ID. *: p <0.05 and ****: $p < 0.0001$ by the two-tailed Student's t-test.

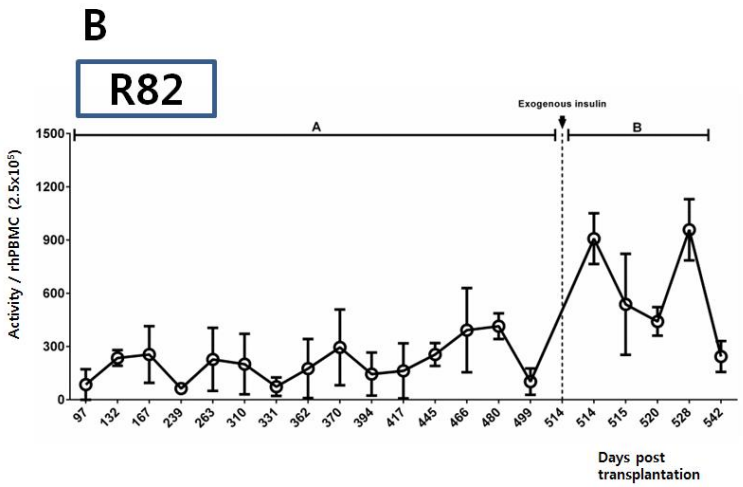

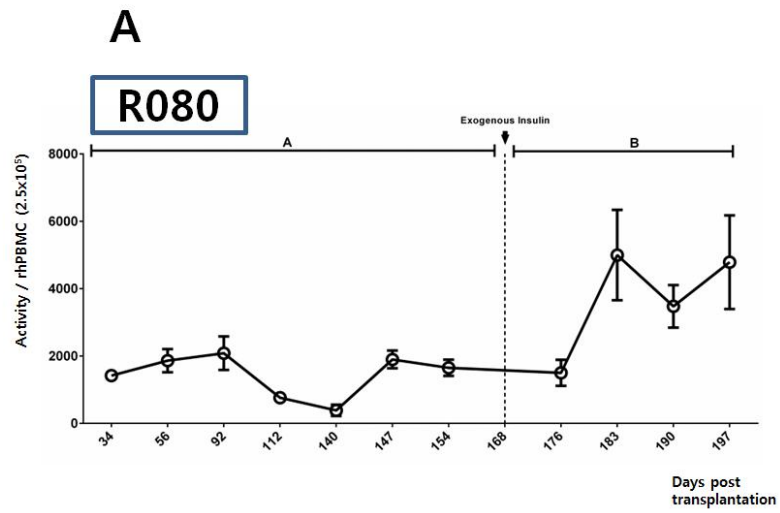

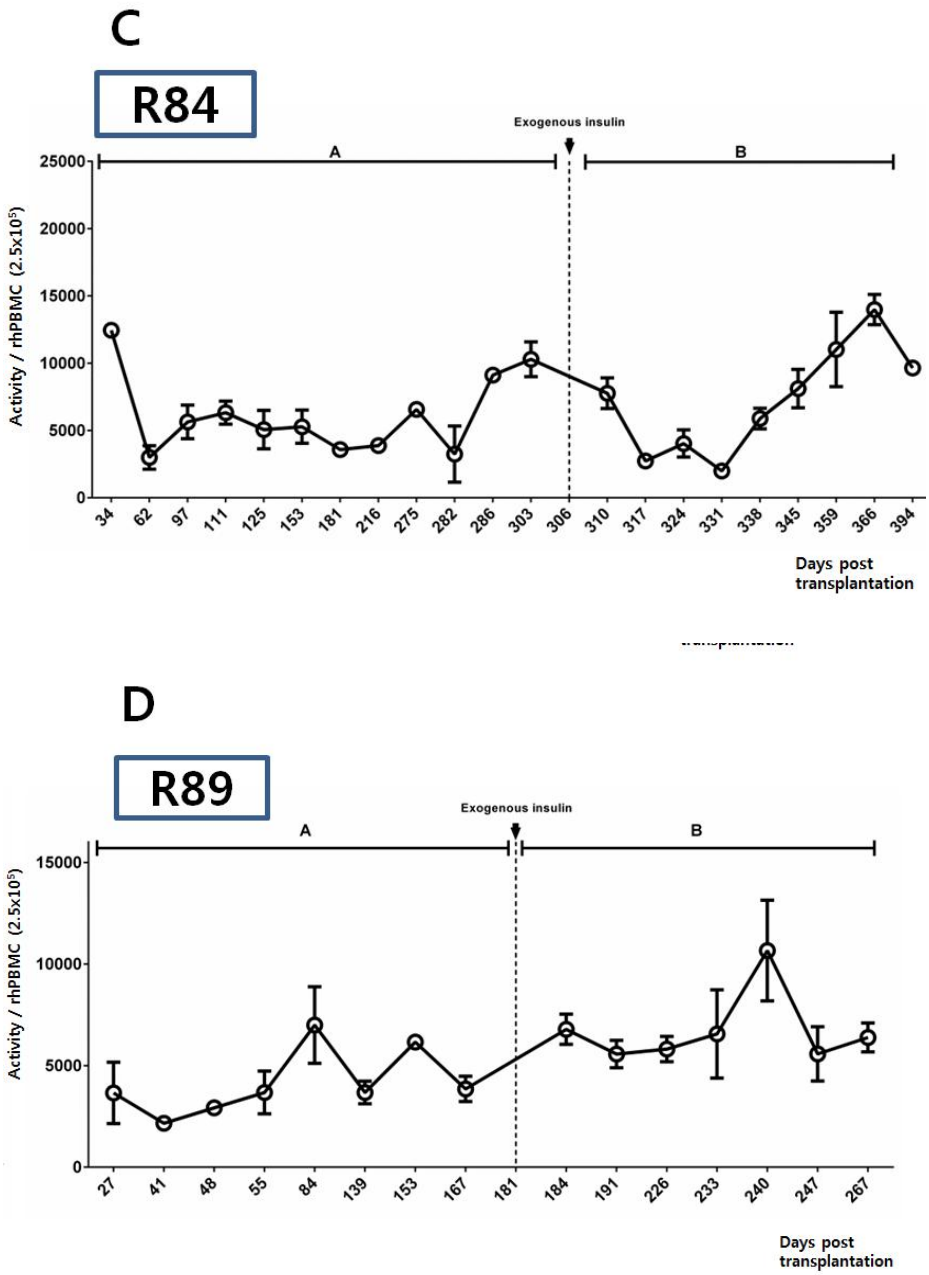

Fig.16. Time-series IFN-γ ELISpot monitoring of long-term graft surviving monkeys by measuring signal intensity (represented as spot activity). Upper numbers indicate monkey ID.

$CD8^+$ T cells are the main producers of IFN-γ. And $CD8^+$ T cells include not only IFN-γ producing effector cells but also non-functional or regulatory $CD8^+$ T cells. Therefore, if the frequency of $CD8^+$ T cells were changed after the rejection, an elevation in the number of spots would be attributed to changes in the number of $CD8^+$ T cells out of total T cells. Also, it is possible that if a significant number of $FoxP3^+$ regulatory T cells were present, they may suppress IFN-γ secretion of the responder cells[60]. Thus, I measured the ratio of $CD4^+/CD8^+$ T cells in the peripheral blood and the percentage of $CD4^+$ $FoxP3^+$ T cells. I found $CD8^+$ T cells to be the predominant T cell population throughout the follow-up period. Moreover, the percentage of $CD4^+$ $FoxP3^+$ T cells did not change meaningfully during the hyperglycemic period (Fig. 17A-D and 18A-D). Thus, neither the ratio of $CD4^+/CD8^+$ T cells nor the percentage of $FoxP3^+$ T cells influenced our results.

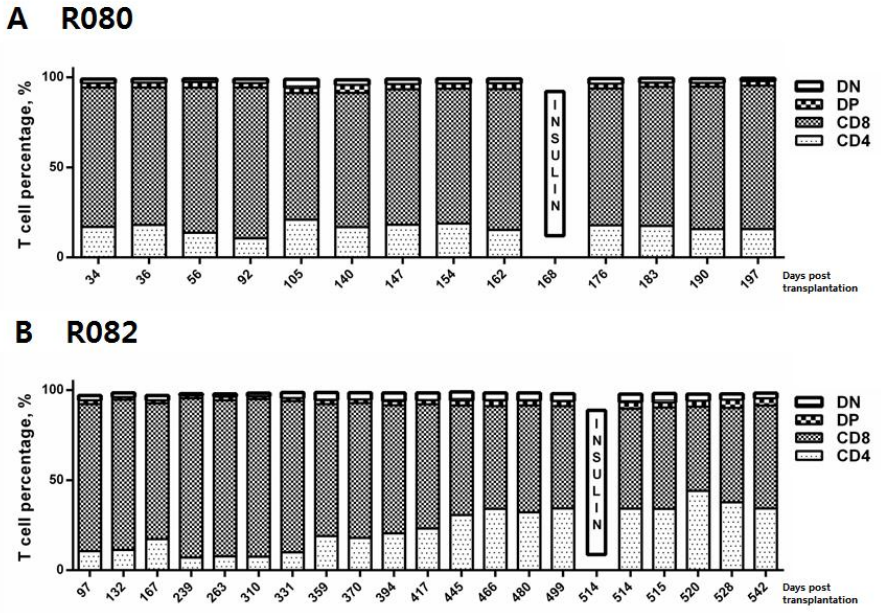

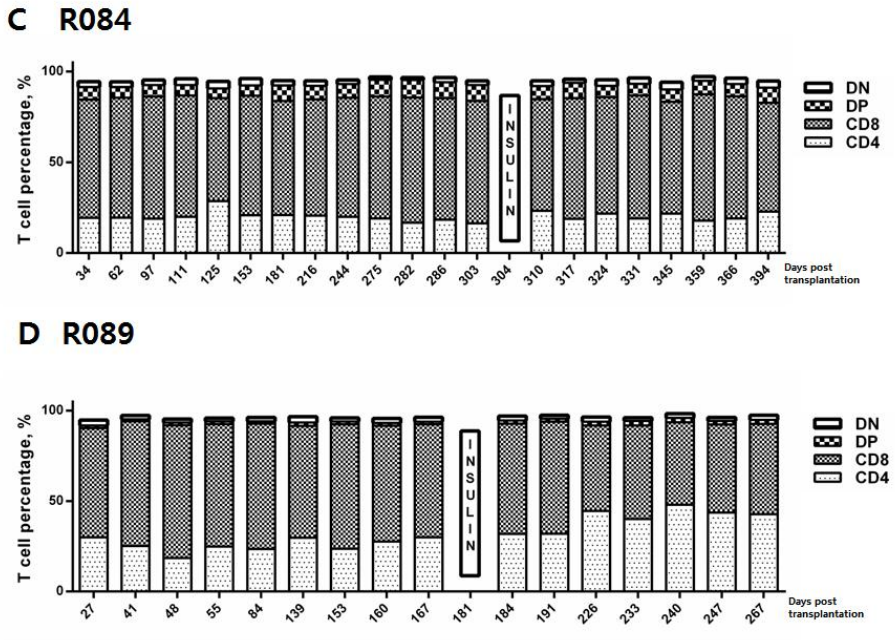

Fig.17. The percentage of CD4 and CD8 subsets in peripheral T cells. Peripheral blood from islet recipient monkeys was obtained periodically before and after graft rejection. To determine the distribution of T cell subsets, peripheral blood cells were stained with fluorescence-conjugated anti-CD3, anti-CD4, and anti-CD8 antibodies. The percentages of each subset among $CD3^+$ cells on indicate days after porcine islet transplantation are depicted sequentially. CD4; % of $CD4^+CD8^-$ cells, CD8; % of $CD4^-CD8^+$ cells, DP; % of $CD4^+CD8^+$ cells, DN; % of $CD4^-CD8^-$ cells among total $CD3^+$ cells, respectively. (A) R080 recipient monkey. (B) R082 recipient monkey. (C) R084 recipient monkey. (D) R089 recipient monkey.

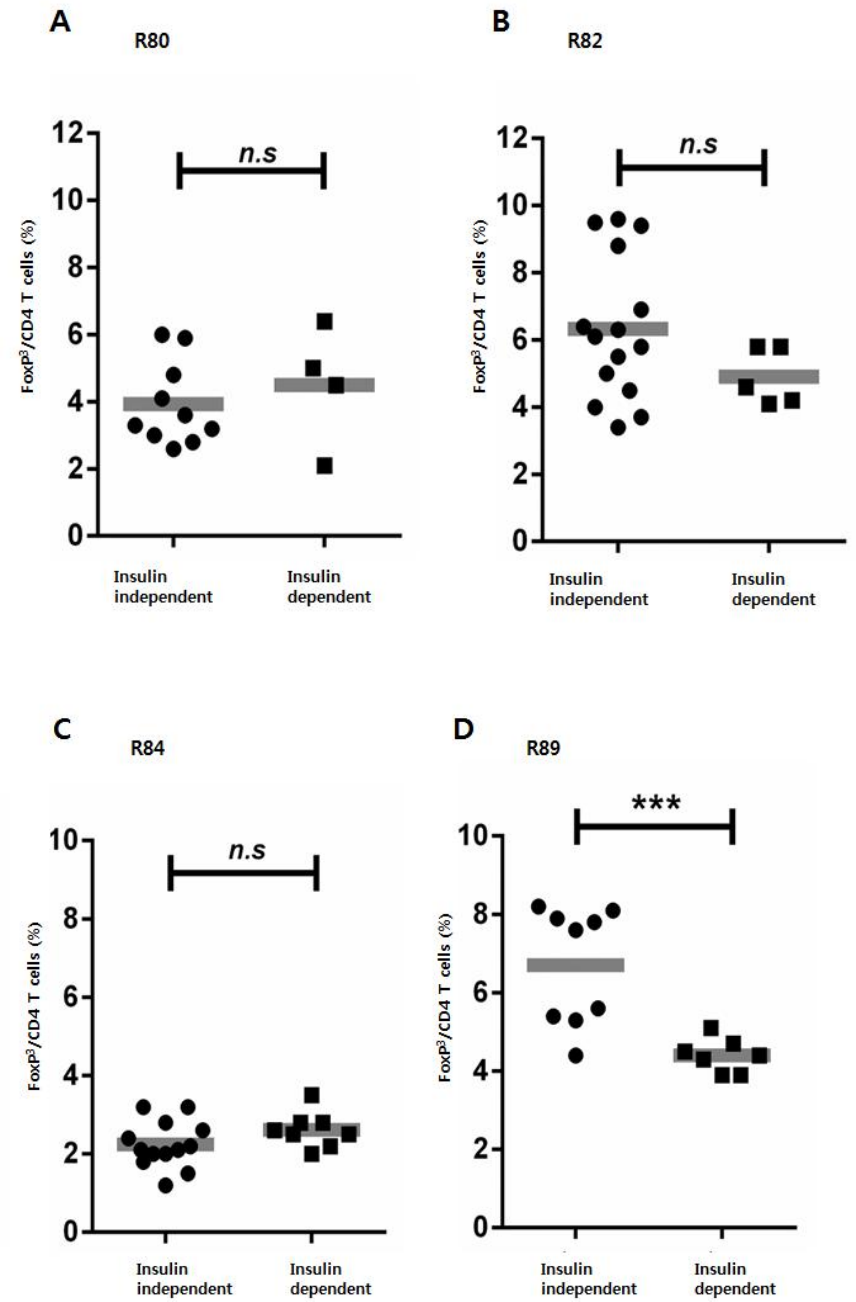

Fig.18. The percentage of FoxP3^{+} regulatory T cells in peripheral blood during the peri-rejection period. Peripheral blood obtained from the islet recipient monkeys during the peri-rejection period was stained with fluorescence-conjugated anti-CD3,

anti-CD4, and anti-FoxP3 antibodies. The percentage of $FoxP3^+$ T cells among $CD3^+CD4^+$ cells was compared between normoglycemia and hyperglycemic periods. (A) R080 recipient monkey. (B) R082 recipient monkey. (C) R084 recipient monkey. (D) R089 recipient monkey. *n.s*; not significant, ***; *P*-value < 0.001

3. Third party islets vs. donor-specific porcine splenocytes as stimulators

Splenocytes from donor pigs were used as stimulators in our ELISpot experiments. Because these results did not 'predict' the rejection of porcine islets, I questioned if stimulation with porcine islet cells would produce more sensitive responses. Although porcine islets from the donors used for the transplantation would be the ideal stimulators, storage of these cells for future use is not practical. Therefore, islets from unrelated pigs were used for the IFN-γ ELISpot assay. As seen in Fig. 19, spot numbers were highly variable even during the early period of transplantation and they did not increase even after the rejection. Therefore, using third party porcine islets as stimulators offers no advantage over donor-specific splenocytes for this assay in adult porcine islet transplantation.

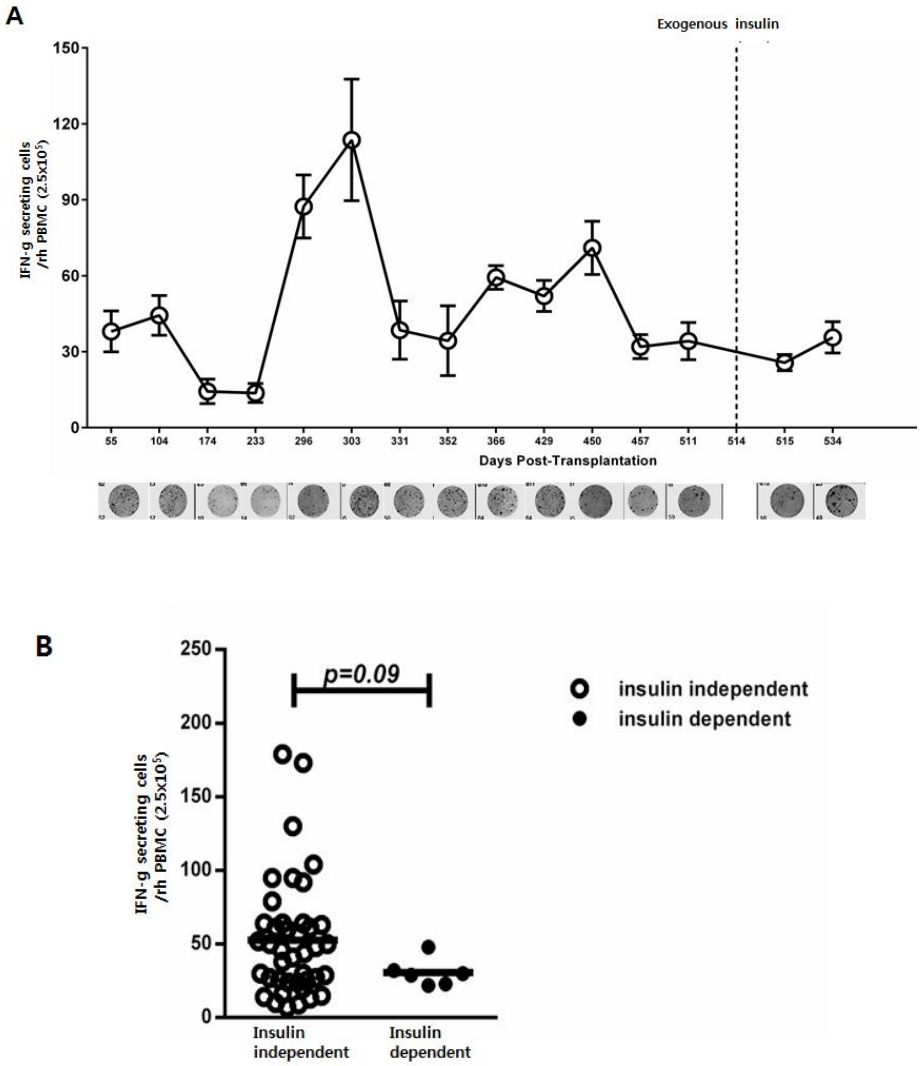

Fig. 19. Sequential ELISpot assay with islet cells from unrelated pigs as the stimulators. Stored PBMCs from the R082 monkey were stimulated with islets from an unrelated pig, and IFN-γ spots were counted. (A) Number of IFN-γ producing spots at various time points was depicted. The day of rejection (estimated by the blood glucose level) is marked with a dotted line. (B) Comparison of the number of IFN-γ producing spots between periods of normoglycemia and hyperglycemia. Bold gray lines represent the mean value of spot numbers during each period. *p*-values were calculated by the two-

tailed Student's *t*-test.

4. Correlation of ELISpot results with cellular infiltration of the graft

Next, I wanted to examine whether the IFN-γ ELISpot results with PBMCs represent cellular rejection at the graft-site. To compare ELISpot results with *in situ* graft situation, liver biopsy samples from recipient monkeys were retrospectively analyzed in both normoglycemic and hyperglycemic periods. During normoglycemia insulin-producing -cells were intact and few $CD3^+$ infiltrating T cells were detected (Fig. 20). However, during the hyperglycemic period, numerous $CD3^+$ infiltrating T cells were present around the islets and destruction of the transplanted islets was observed. Minimal infiltrations of $CD68^+$ cells were detected in both normoglycemia and hyperglycemia periods. These results suggest that significant increases in the number of IFN-γ ELISpot obtained from PBMCs have the possibility to reflect the immune-mediated destruction of islet grafts by T cells.

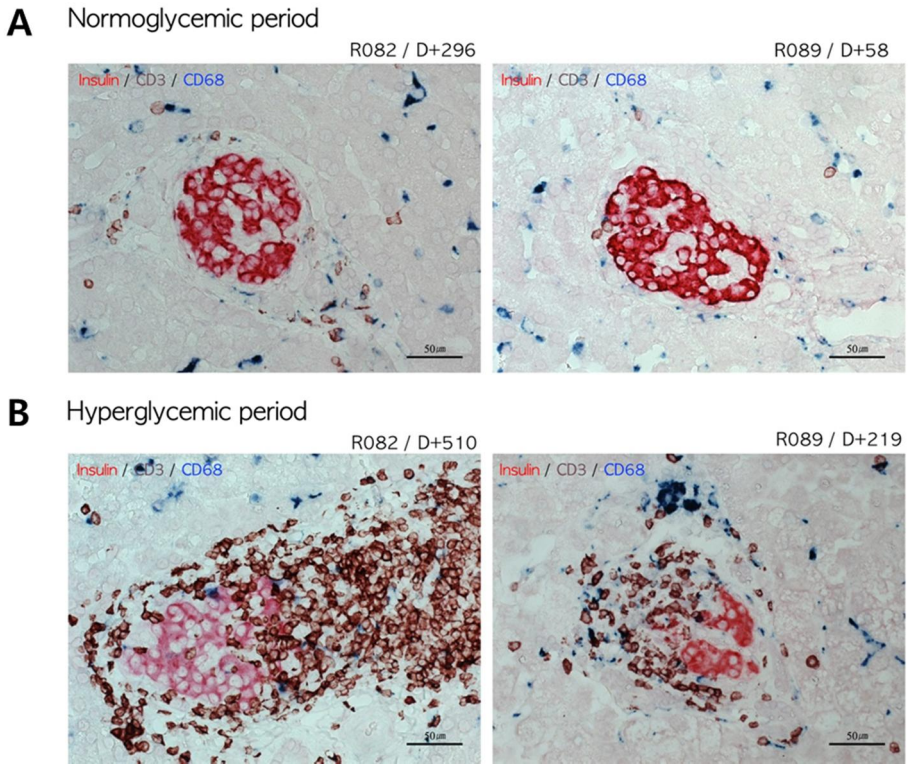

Fig.20. Immunohistochemical examination of the islet graft site. Liver biopsy samples from recipient monkeys during the normoglycemic and hyperglycemic periods were evaluated Sections (4μm) were stained with anti-insulin, anti-CD3, and anti-CD68 antibodies with appropriate secondary antibodies to reveal islet β-cells (red), $CD3^+$ T cells (brown), and $CD68^+$ macrophages (blue). Representative images taken during periods of normoglycemia (upper panels) and hyperglycemia (lower panels) are displayed. Upper-right numbers indicate monkey ID and the day post-transplantation.

DISCUSSION

With the recent revolution in gene editing technology[61] and promising pre-clinical results in islet[24], cornea[62], and heart[63], the clinical application of xenotransplantation is anticipated. Here, I established an immune monitoring procedure that is useful for clinical islet xenotransplantation: a porcine antigen-specific IFN-γ ELISpot assay using PBMCs. The optimal number of the responder cells in this assay was determined to be 2.5×10^5 cells, a finding similar to previous reports[34,64]. In our experiments, un-sensitized rhesus T cells (2×10^5) produced approximately 100 IFN-γ spots (Fig. 13A). Therefore, I could say that the IFN-γ producing precursor frequency of porcine antigen-specific rhesus T cells lies between 1×10^3 and 1×10^4 in our setting. Considering that the general precursor frequency of human T cells to porcine PBMCs measured by mixed leukocyte reaction assay ranges from 1 to 10%[65], and not all proliferating cells can secret IFN-γ, our results are within the expected outcome. In addition, our results suggest that using more than 2.5×10^5 responder rhesus PBMCs would produce too many IFN-γ spots. In our experiments, $CD8^+$ T cells were the main producers of IFN-γ (Fig. 13D), and further provision of agonist CD28 co-stimulation had no effect (Fig. 13C). This suggests that the production of IFN-γ by porcine antigen-specific, rhesus $CD8^+$ T cells occurs independently of a CD28 co-stimulation. It is known that the reactivation of memory $CD8^+$ T cells does not depend on CD28[66-68]. Hence, the IFN-γ producing $CD8^+$ T cells in our experiments could be interpreted as porcine antigen-reactive memory $CD8^+$ T cells.

In clinical organ transplantation, there is a need for an appropriate method to monitor and predict undesired immune responses to the graft. By measuring the level of donor-

specific antibody (DSA), antigen-specific humoral immune responses can be monitored. This DSA measurement can be used to predict rejection of the transplanted organs[69,70]; however, monitoring of antigen-specific cellular immune responses has not been commonly used. In this context, I presumed that sequential monitoring of antigen-specific cellular immune responses using our IFN-γ ELISpot method may be predictive of cellular rejection. However, I only observed a significant increase in antigen-specific IFN-γ producing cells after overt graft rejection by T cells, which was defined by the immunopathology of the biopsied graft site (Fig. 20A-B). The failure to predict T cell-mediated graft rejection using the ELISpot assay may have been due to the extremely low numbers of porcine antigen-specific T cells in PBMCs during the early stages of cellular rejection. Alternatively, the major antigenic determinant might have been porcine islet-specific antigens that are presented by the indirect pathway[71] because our recipient PBMC co-cultured with donor splenocytes assay was able to reflect mainly direct pathway. To overcome the limitation described above, I am planning to set up a more sensitive protocol by the addition of autologous monocyte.

Another limitation of our study is that no pre-transplant assay results were described. Actually, I had 2 pre-transplant PBMC samples (R082, R089) at the time of assay (data not shown). However, I did not include the pre-transplant ELISpot results as a control because the number of cases was too small to have a statistical significance. The increase of the number of pre-transplant samples will fortify the validity of porcine antigen-specific IFN-r ELISpot as a tool for monitoring cellular immune response in nonhuman primate model.

ELISpot analysis using third party porcine islets as stimulators failed to show any

correlation with graft outcome at all (Fig. 19A-B.). This suggests that the T cells contributing to the graft rejection respond to donor-specific (islet-non-specific) antigens rather than tissue (islet) – specific antigens.

In conclusion, I established an ELISpot assay for the assessment of porcine antigen-specific IFN-γ producing cells within PBMCs. ELISpot analysis of time-series PBMC samples from monkeys transplanted with porcine islets confirmed that donor antigen-specific immune responses could be effectively monitored by the ELISpot assay, reflecting T cell infiltration into the graft. Further studies will be required to improve this ELISpot assay in order to predict cell-mediated graft rejection before overt rejection of the graft.

PART 3

Bioinformatics analysis combined with peripheral blood RNA-sequencing unveiled insidious immune rejection in the chronic phase after pig-to-nonhuman primate islet xenotransplantation

INTRODUCTION

Since Edmonton protocol in islet transplantation was introduced in 2000[72], human pancreatic islet transplantation has become an established treatment option to treat some selected type 1 diabetic patients who frequently experience fatal hypoglycemic unawareness. Although the result of long-term islet graft function after islet transplantation has been improved, still over half of the patients transplanted with human islet turned to be insulin dependent state within 5 years[49,73]. The causes for this chronic islet graft loss are controversial; both immunological and non-immunological events take place in the chronic phase, leading to significant islet loss. They encompass a higher rate of islet apoptosis due to ER stress[74,75], hypoxia[76,77] in end-portal venules in the liver, and recurrent autoimmunity[78]. In addition, there is evidence of metabolic deterioration due to lipid accumulated around the islets (lipotoxicity)[79,80] and toxicity of immunosuppressive drugs[81,82]. A significant portion of islet transplants undergo chronic failure due to immune rejection, but none of the above can clearly explain the exact cause of chronic islet graft loss.

Recently, I have demonstrated consistent results of long-term pig islet graft survivals $\geq$ 6 months in five independent monkeys. This result is important, because the pig islets are relatively easily susceptible to various stresses such as ER stress, hypoxia, and inflammation than islets from other species[83] and even they are present in metabolically hostile host environment (pig-to-NHP metabolic incompatibility)[84] This unique opportunity allows us to examine how the pig islets are lost in the chronic phase after islet transplantation into the monkeys. Here, I selected two monkey recipients; one (R051) had stable graft function for entire follow-up periods and the other (R080)

lost graft function around DPT 160. I sought to find the difference of RNA signatures in peripheral blood between two recipients and pinpoint the cause of early islet graft loss in R080 by a highly innovative bioinformatics tool.

MATERIALS AND METHODS

1. Animals

Two rhesus monkeys (R051, R080) were used in our study.

2. IVGTT

After an overnight fasting without insulin, 0.5 g/kg of 50% dextrose solution was added to the same volume of normal saline was infused intravenously for 1 min. Blood glucose levels were measured in monkeys before and 2, 5, 15, 30, 60, 90, and 120 min after infusion. Insulin and c-peptide levels were measured at the same time intervals.

3. ELISPOT assay:

ELISPOT analysis was performed by the method previously described[40]. 2.5×10^5 monkey PBMCs were cultured with 5×10^5 porcine splenocytes (30Gy irradiation). The resulting spots were counted on a computer-assisted ELISpot Reader System (AID, Straßberg, Germany).

4. RNA sequencing

Total RNA from peripheral blood of Rhesus monkey was extracted using the Ambion Ribopure™-Blood kit (Life technologies). 500 μL of Rhesus monkey peripheral blood was collected and 1.3mL RNA*later*™ solution was added to the blood sample. After 13,000 ×*g*, room temperature, for 1 min of centrifugation, the supernatant was removed by aspiration. 800μL of Lysis solution and 50μL of Sodium Acetate solution was added to the cell pellet from RNA*later*-stabilized sample. To lyse the blood cells,

the sample was mixed by vigorous vortexing. Then, 500μL of Acid-Phenol: Chloroform was added and the sample was shaken vigorously for 30 seconds. The mixture was stored at room temperature for 5 min. After 5 min, to separate aqueous phase, 13,000 x g, room temperature, for 1 min of centrifugation was conducted. The aqueous phase that containing RNA was transferred to a new 2mL-microtube. 600μL of 100% ethanol was added to the sample and the tube was mixed briefly but thoroughly. Next, the sample was applied to a RNA Filter Cartridge. The sample containing RNA passed through the filter and RNA was captured in the filter. Then the filter was washed twice by 700μL of Wash solution. After that RNA in the filter was eluted by 50μL of RNase-free ddH_2O preheated to 75°C. Eluted total RNA was stored in -80°C. Next, RNA sequencing was performed. Purified total RNA was sequenced by the Theragen etex (Seoul, South Korea).

5. Biopsy and Immunohistochemistry

Biopsy and immune-histochemical staining were conducted as described previously[24]. Briefly, liver biopsy samples from recipient monkeys were fixed in 10% neutral buffered formalin, and embedded in paraffin. Paraffin-embedded tissues were sectioned at 4μm using a microtome. Each de-paraffinized and hydrated section was incubated 30min with primary antibody cocktail for insulin (Santa Cruz Biotechnologies) and CD3 (DAKO), insulin and CD4 (Santa Cruz Biotechnologies), or insulin and CD8 (Abcam, Cambridge, UK), and then wash four times in TBST. After staining procedure, all of the stained slides were dried at 60℃ and mounted with aqueous mounting medium (Thermo scientific). The stained sample was observed by

Carl Zeiss Axio Imager A1 microscope and images were taken with a micrograph with AxioVision software (Carl Zeiss).

6. Statistics

The statistical software GRAPHPAD PRISM5 (GraphPad Software, Inc., La Jolla, CA) was used for Student's t-test with two-tailed *P*-value and Fisher's exact test was used for categorizing GLPAPs.

RESULTS

Peripheral blood RNA sequencing was carried out to find cause(s) of graft loss in the chronic phase

I recently reported long-term survivals after adult porcine islet xenotransplantation in five independent monkeys[24]. One (R051) showed complete normal glycemia and glucose tolerance after islet transplantation for entire follow-up periods, whereas the other (R080) experienced relatively early hyperglycemia around DPT 160, reflecting a graft failure (Fig. 21A-B). Intra-venous glucose tolerance test (IVGTT) indeed showed that the pig islet graft loss in R080 was in progress between DPT120 and 180 (Fig. 21C-D). In this period, I performed routine laboratory examinations including vital sign, complete blood cell count (CBC), liver function test (LFT), C-reactive protein (CRP), kidney function test (blood urine nitrogen/creatinine), electrolyte panel (sodium, potassium and chloride), lipase and amylase. However, no abnormal data were obtained. Also, immune monitoring of peripheral blood lymphocyte subsets by FACS, titer of donor-specific antibody by ELISA, peripheral blood cytokine level by cytometric bead assay did not reveal any noticeable change (data not shown). Finally, I conducted porcine-antigen-specific IFN-γ ELISpot assay, which has been widely used to monitor antigen-specific allo-reactive T cell responses in humans[58,59]. However, only after overt graft failure (DPT 197), the number of porcine antigen-specific IFN-γ secreting cells in PBMCs significantly increased (Fig. 21E). Because I were not able to find the exact cause(s) for graft loss pre- and during the hyperglycemic period in R080, I performed RNA sequencing in whole blood samples taken at four different time points from graft-losing R080 vs. graft stable R051 (Fig. 21F).

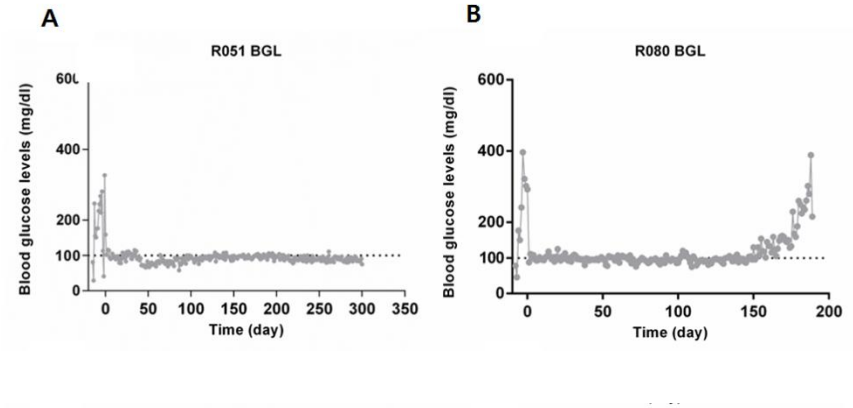
A
R051 BGL
Blood glucose levels (mg/dl)
Time (day)
B
R080 BGL
Blood glucose levels (mg/dl)
Time (day)

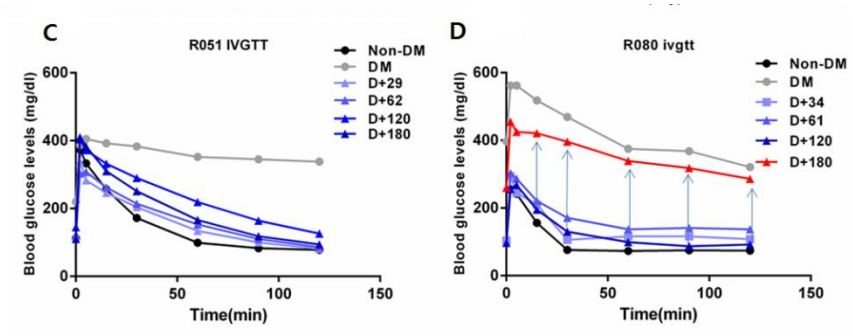
C
R051 IVGTT
Non-DM
DM
D+29
D+62
D+120
D+180
Blood glucose levels (mg/dl)
Time(min)
D
R080 ivgtt
Non-DM
DM
D+34
D+61
D+120
D+180
Blood glucose levels (mg/dl)
Time(min)

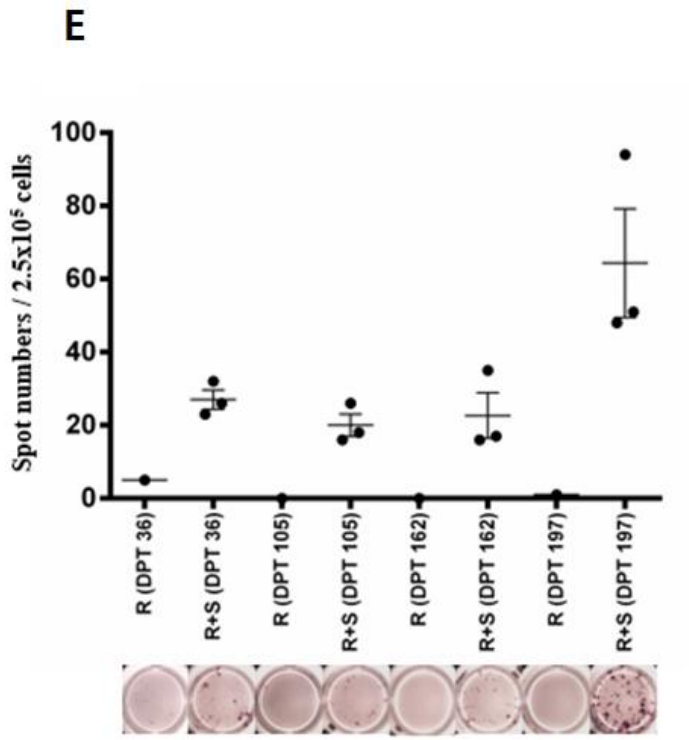
E
Spot numbers / 2.5x10⁵ cells
R (DPT 36)
R+S (DPT 36)
R (DPT 105)
R+S (DPT 105)
R (DPT 162)
R+S (DPT 162)
R (DPT 197)
R+S (DPT 197)

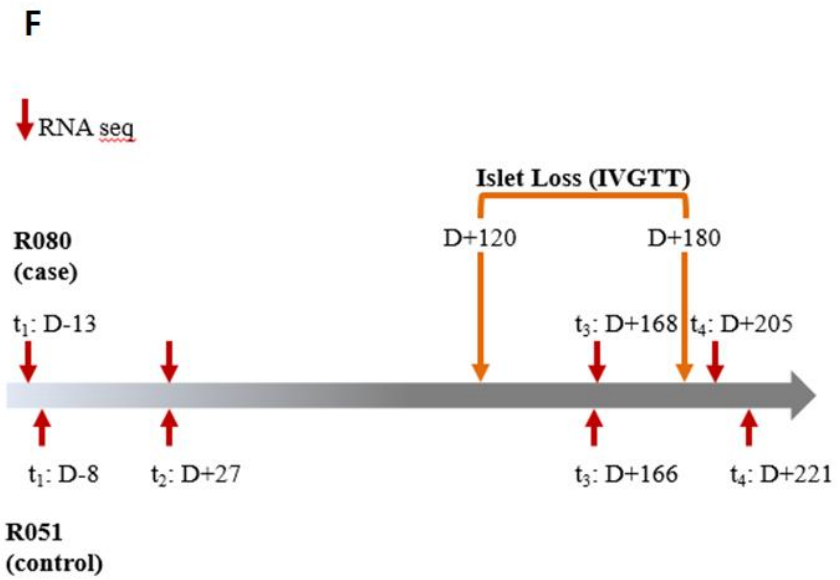

Fig.21. Graft function and cell-mediated immune status monitoring and experimental scheme. (A-B) Blood glucose level of R051 and R080. R080 showed an insidious increase of blood glucose level around DPT 150 (C-D) IVGTT results of R051 and R080. Between DPT 120 and 180, R080 demonstrated prominent glucose intolerance. (E) IFN-γ ELISpot of R080, R: Responder only, R+S: Responder + Stimulator. Until before DPT 197, porcine antigen-specific IFN-γ producing cells were not increased in the peripheral blood. (F) Sampling time point for RNA sequencing. Whole blood achieves were used for RNA sequencing. (t_1: before transplantation, t_2: one month after transplantation, t_3: immediate after increase of blood glucose in R080 and corresponding time point for R051, t_4: after overt hyperglycemia in R080 and corresponding time point for R051)

Graft loss period-related activated pathways (GLPAPs) can be outstanding from Kyoto Encyclopedia of Genes and Genomes (KEGG) in R080 at the time of

immediate after increase of blood glucose (t3)

After confirming the validity of RNA-sequencing (RNA-seq) raw data, I used a novel bioinformatics tool called Time-series RNA-seq Analysis Package (TRAP)[85] to determine which pathways play roles in graft loss process (Fig. 22). Because the t_2 and t_3 represent graft-maintaining and graft-losing period, respectively in R080, I focused on these time points and selected pathways as follows: i) select up-regulated pathways with p-value under 0.05 from the results yielded by comparing the t_2 and the t_3 in R080 by TRAP algorithm, ii) select up-regulated pathways with p-value under 0.05 from the results yielded by comparing R080 and R051 at the t_3 and then take pathways belonging to the intersection of those sets (Fig. 23). By doing so, I could obtain 59 pathways among 287 pathways in KEGG Rhesus database and these pathways were dubbed GLPAPs as can be seen in table 2.

After obtaining 59 of GLPAPs, I was able to calculate p-values for each category of the pathways using Fisher's exact test to determine how significantly GLPAPs were enriched in each category. To calculate p-values, I constructed contingency table with two variables; TRAP result set and category. Each cell of the table was filled by a number of the pathways according to the standard whether if the pathway belongs to the category or not and if the pathway belongs to the TRAP result set or not (Fig. 24.). The p-values for each category are shown in table 3. Surprisingly, the most enriched category was found to be "immune system" despite I did not find any perturbation of immunological parameters in the routine immune monitoring system. This finding strongly implies that immunological responses are somehow activated and ongoing during t_3 in R080 compared to t_2 in R080 and corresponding time points in R051.

Pathway	Name	Category
mcc04062	Chemokine signaling pathway	Immune system
mcc04611	Platelet activation	
mcc04620	Toll-like receptor signaling pathway	
mcc04621	NOD-like receptor signaling pathway	
mcc04623	Cytosolic DNA-sensing pathway	
mcc04650	Natural killer cell mediated cytotoxicity	
mcc04660	T cell receptor signaling pathway	
mcc04662	B cell receptor signaling pathway	
mcc04664	Fc epsilon RI signaling pathway	
mcc04670	Leukocyte transendothelial migration	
mcc04010	MAPK signaling pathway	Signal transduction
mcc04012	ErbB signaling pathway	
mcc04022	cGMP-PKG signaling pathway	
mcc04064	NF-kappa B signaling pathway	
mcc04068	FoxO signaling pathway	
mcc04070	Phosphatidylinositol signaling system	
mcc04152	AMPK signaling pathway	
mcc04370	VEGF signaling pathway	
mcc04630	Jak-STAT signaling pathway	
mcc04668	TNF signaling pathway	
mcc04910	Insulin signaling pathway	Endocrine system

mcc04915	Estrogen signaling pathway	
mcc04917	Prolactin signaling pathway	
mcc04918	Thyroid hormone synthesis	
mcc04919	Thyroid hormone signaling pathway	
mcc04921	Oxytocin signaling pathway	
mcc03013	RNA transport	Translation
mcc04210	Apoptosis	Cell growth and death
mcc04961	Endocrine and other factor-regulated calcium reabsorption	Excretory system
mcc04970	Salivary secretion	Digestive system
mcc05211	Renal cell carcinoma	Cancers: Specific types
mcc05212	Pancreatic cancer	
mcc05213	Endometrial cancer	
mcc05214	Glioma	
mcc05215	Prostate cancer	
mcc05219	Bladder cancer	
mcc05220	Chronic myeloid leukemia	
mcc05221	Acute myeloid leukemia	
mcc05223	Non-small cell lung cancer	
mcc04141	Protein processing in endoplasmic reticulum	Folding, sorting and degradation
mcc04320	Dorso-ventral axis formation	Development
mcc04380	Osteoclast differentiation	

mcc04540	Gap junction	Cellular communication
mcc04810	Regulation of actin cytoskeleton	Cell motility
mcc04722	Neurotrophin signaling pathway	Nervous system
mcc04725	Cholinergic synapse	
mcc04060	Cytokine-cytokine receptor interaction	Signaling molecules and interaction
mcc05142	Chagas disease (American trypanosomiasis)	Infectious diseases: Parasitic
mcc05143	African trypanosomiasis	
mcc05144	Malaria	
mcc05161	Hepatitis B	Infectious diseases: Viral
mcc05162	Measles	
mcc05164	Influenza A	
mcc05166	HTLV-I infection	
mcc05168	Herpes simplex infection	
mcc05169	Epstein-Barr virus infection	
mcc05200	Pathways in cancer	Cancers: Overview
mcc05203	Viral carcinogenesis	
mcc05205	Proteoglycans in cancer	

Table 2. Graft losing period-related activated pathways (GLPAPs). Fifty-nine out of two hundred-eighty-seven pathways in rhesus KEGG database were selected after applying of TRAP algorithm.

Category	P-value
Immune system	0.0001962
Cancers: Specific types	0.0003236
Infectious diseases: Viral	0.0003591
Signal transduction	0.0120207
Infectious diseases: Parasitic	0.1036661
Endocrine system	0.1076348
Development	0.1083940
Cell motility	0.2055749
Cancers: Overview	0.2132333
Digestive system	0.6910951
Nervous system	1.0000000
Cell growth and death	1.0000000
Cellular communication	1.0000000
Excretory system	1.0000000
Folding, sorting and degradation	1.0000000
Signaling molecules and interaction	1.0000000
Translation	1.0000000

Table 3. Significantly enriched categories of GLPAPs Categories are listed in ascending order of p-values calculated by Fisher's exact test. Immune system category pathways were highly enriched.

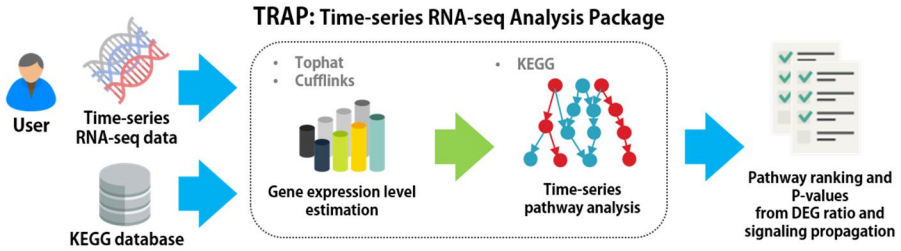

Fig.22. Brief introduction of TRAP[85]. If time-series RNA-seq data were analyzed by TRAP, pathway rankings and p-values in KEGG database were calculated according to the algorithm.

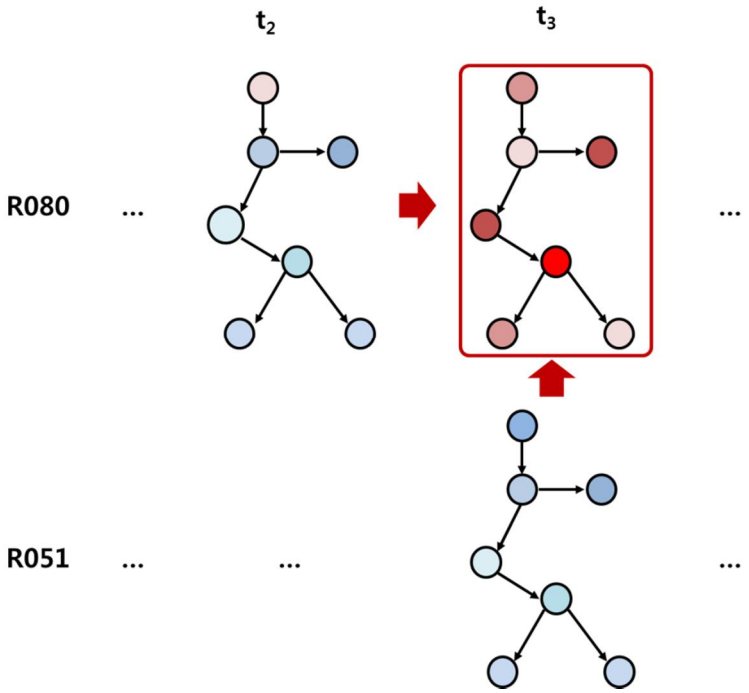

Fig. 23. Pathway filtering strategy. GLPAPs were selected by taking the intersection of two TRAP results. One was to detect which pathways were activated at t_3 compared to t_2 in R080. The other was to detect which pathways were activated in R080 compared to R051 at t_3.

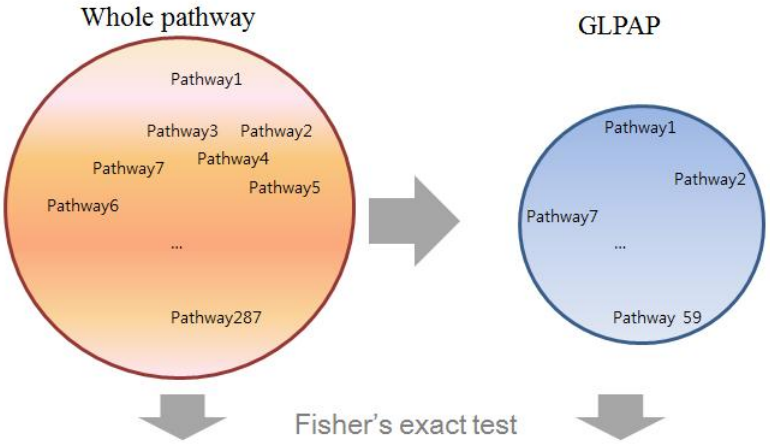

	GLPAP	Non GLPAP	Total set
Concerned Category	A	B	A+B
Not concerned Catetory	C	D	C+D
Total pathways	A+C = 59	B+D = 228	A+B+C+D=287

Fig.24. A contingency table with two variables to calculate p-values of each category. To calculate GLPAP enrichment for each category of pathways, I built contingency tables for each category according to the two variables. One is whether a pathway is GLPAP or not and the other is whether a pathway belongs to the concerned pathway.

Pathway cross-talk network was constructed

Biological pathways participate in biological processes by constituting a network. Even though I found that the pathways categorized in immune system were the most enriched after GLPAPs filtering, I was not able to pinpoint specific pathways, which are responsible for graft loss. Therefore, it would be desirable to analyze networks of the pathways to find out the most communicative pathways to induce graft loss among GLPAPs. To this end, I constructed a crosstalk network of the activated pathways and used the pathway information of KEGG[86] to connect the edge between the pathways; pathway and gene link information was acquired using KEGG API and neighboring

pathway information, parsing KEGG Markup Language (KGML) files. I considered that any two pathways were connected if the following conditions were satisfied: i) two pathways have at least one overlapping gene; ii) two pathways are neighbors to each other. It is one of the well-studied methods to connect an edge between two pathways in a pathway cross-talk network based on the overlapping genes[87-89]. I also added one more condition to prune the edges as follows: Firstly, I enumerated all edges between the pathways and aggregated all genes that belong to the pathways at the both ends of each edge. Then, I tested the significance of each edge using paired t-test on the differential expression level of the summed genes between t_3 of R080 and R051 (Fig. 25). By doing so, I was able to calculate p-values for every edge in the network and prune the edges if the p-value was over 0.05.

Next, I focused on the cross-talk network. I visualized the network using Cytoscape[90] (Fig. 26). There were 54 pathways out of 59 in TRAP result set connected by 158 edges in the network. I calculated closeness centrality for every node and sorted the nodes by the centrality in descending order to analyze which pathways played a central role in the network to induce the biological response at t_3 of R080. I primarily considered the pathways with the centrality equal to or bigger than 0.45 (Immune system category) or 0.50 (signal transduction category) were meaningful. There were seven pathways of immune system category that met the criterion (table 4). The pathways were Toll-like receptor signaling pathway, NOD-like receptor signaling pathway, B cell receptor signaling pathway, T cell receptor signaling pathway, chemokine signaling pathway and natural killer cell-mediated cytotoxicity Fc epsilon RI signaling pathway in descending order of the centrality. Likewise, MAPK signaling pathway and JAK-STAT signaling pathway of signal transduction category met the

criterion (table 5). These two pathways were also the first and the third highest pathway in terms of closeness centrality in the network.

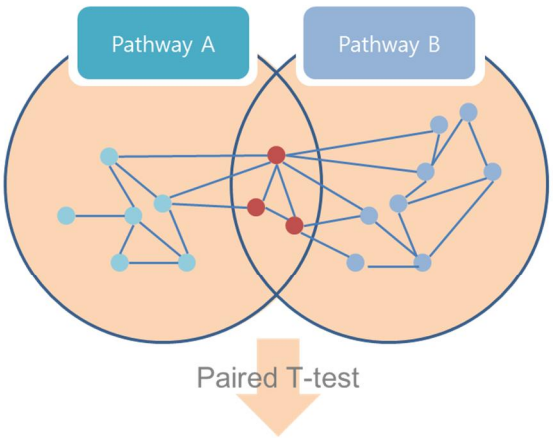

Edge Connection if p-value < 0.05
Gene Expression level of $R080_{t3}$ (A∪B) vs Gene Expression level of $R051_{t3}$ (A∪B)

Fig.25. Edge connection strategy. For each possible crosstalk pair of pathways, I conducted paired t-test to see how the crosstalk of pathways was significantly activated in R080 compared to R051.

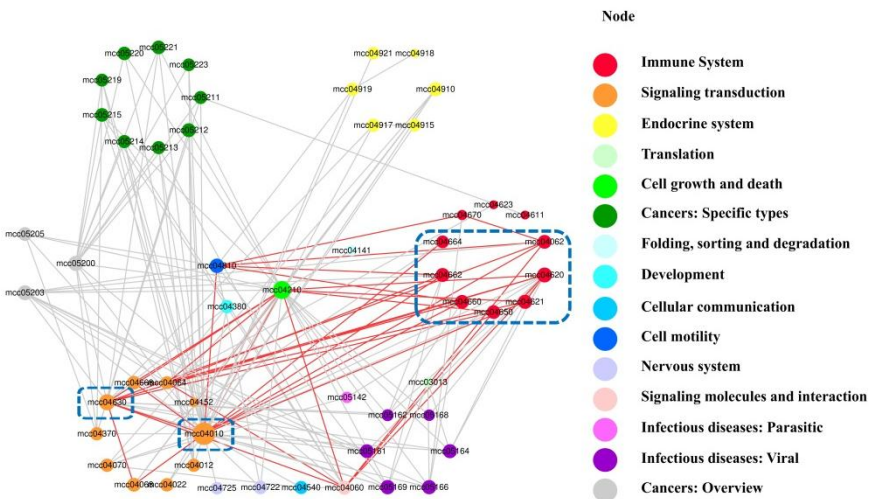

Fig.26. Pathway crosstalk network. Nodes and edges of network consisted of GLPAPs were demonstrated at t_3 of R080 according to crosstalk network building strategy. Blue dotted rectangles represent pathways of high closeness centrality score in the immune system and signal transduction category. Small characters inside of the node represent KEGG pathway IDs. Seven pathways of immune system category and two pathways of signal transduction pathways were noticed.

PathwayID	**Pathway Name**	**Closeness Centrality**
mcc04620	**Toll-like receptor signaling pathway**	**0.5353535**
mcc04621	**NOD-like receptor signaling pathway**	**0.5047620**
mcc04662	**B cell receptor signaling pathway**	**0.5000000**
mcc04660	**T cell receptor signaling pathway**	**0.4953271**
mcc04062	**Chemokine signaling pathway**	**0.4953271**
mcc04650	**Natural killer cell mediated cytotoxicity**	**0.4907407**
mcc04664	**Fc epsilon RI signaling pathway**	**0.4568966**
mcc04670	Leukocyte transendothelial migration	0.3680556
mcc04611	Platelet activation	0.3212121
mcc04623	Cytosolic DNA-sensing pathway	0.3192771

Table 4. Closeness centrality for pathways of the immune system. Each pathway in immune system category was listed in ascending order of closeness centrality calculated from cytoscape.

PathwayID	Pathway Name	Closeness Centrality
mcc04010	**MAPK signaling pathway**	**0.80303030**
mcc04630	**Jak-STAT signaling pathway**	**0.57608696**
mcc04068	FoxO signaling pathway	0.49532710
mcc04668	TNF signaling pathway	0.49074074
mcc04022	cGMP-PKG signaling pathway	0.48181818
mcc04370	VEGF signaling pathway	0.47747748
mcc04070	Phosphatidylinositol signaling system	0.47747748
mcc04012	ErbB signaling pathway	0.47321429
mcc04064	NF-kappa B signaling pathway	0.46491228
mcc04152	AMPK signaling pathway	0.33544304

Table 5. Closeness centrality for pathways of signal transduction. Each pathway in signal transduction category was listed in ascending order of closeness centrality calculated from cytoscape.

Immune rejection of the pig islets by mostly $CD3^+$ T was found in liver biopsy sample from R080

The results from bioinformatics analyses on RNA-seq suggested that immune rejection toward the pig islets is insidiously in progress between DPT120 and DPT180 and several key activated pathways during this processes are outstanding in RNA signatures of the peripheral blood. Finally, I wanted to confirm whether our novel bioinformatics analysis reflected 'real' biological processes. I collected liver biopsy samples at DPT184 from R080 and examined graft histology by

immunohistochemistry. Indeed, I found that insulin positive islet grafts were heavily infiltrated by mostly $CD3^+$ T cells and some $CD68^+$ macrophages (Fig. 3-7). Because I did not find any noticeable changes in peripheral immune cells phenotyping, antibody titers, cytokines and other routine laboratory tests, I can conclude that bioinformatics analyses on peripheral blood RNA seq. tell us whether immunological reaction in response to the graft is in progress or not and furthermore, which biological pathways are activated during this process in the transplant recipient.

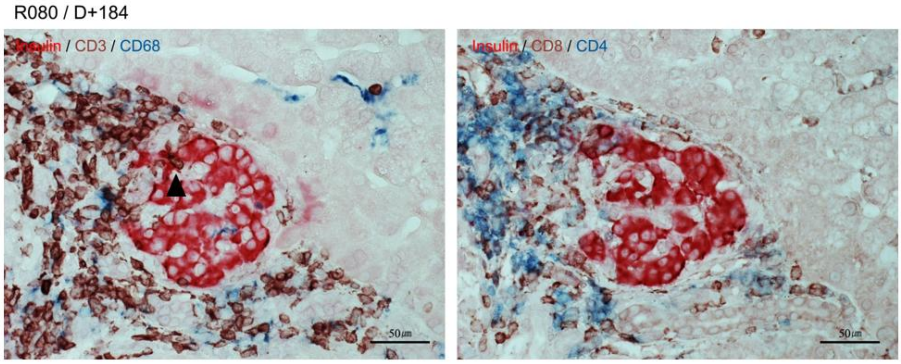

Fig.27. Histology of islet xenografts. R080's grafts were heavily infiltrated by several types of immune cells. Immune cells largely consisted of $CD3^+$ T cells. Both $CD4^+$ and $CD8^+$ cells infiltrated near the graft. $CD68^+$ cell was also observed. Black arrow indicated intra-graft infiltration of $CD3^+$ T cell.

DISCUSSION

Over the past 30 years after introduction in the clinics[91], human islet transplantation is now considered an accepted and reimbursed clinical care[92]. Although it is successful in short-term, it lacks long-term durability, resulting in most patients transplanted with islets returning to insulin dependency. Similarly, I found that the pig islet graft was also lost in some of the transplant recipient monkeys within 6~30 months after transplantation in pig-to-NHP islet xenotransplantation. This unique opportunity allows us to test whether pig islet graft was lost due to either immune rejection or other non-immunological events such as metabolic stress, drug toxicity or apoptosis.

Because I did not find any definitive evidence of immune rejection in routine laboratory tests including biochemical and immunological assays in peripheral blood from R080, I had to introduce an innovative bioinformatics tool based on RNA-seq data obtained from whole blood taken at various time points after transplantation in parallel to performing similar experiments on control animal (R051). Fortunately, I found a suitable bioinformatics data analysis package called TRAP. It was originally developed to find out time-series activated pathways in KEGG database. I decided to adopt TRAP to analyze our big data. Interestingly, several pathways (GLPAPs) were activated t_3 in R080 compared to t_2 in R080. By adding a step of comparing t_3 in R080 to t_3 in R051, I was able to validate these results and prune noisy pathways. Furthermore, I determined to categorize the activated pathways in KEGG database. Surprisingly, I found that the pathways categorized as immune system were the highest enriched.

Next, I focused on the specific pathways among GLPAPs. By using cross-talk network construction, 9 out of 59 pathways were noticed. I considered that these pathways were somehow involved in the deterioration of chronic graft loss in our primate experiment. Even though I were not able to determine the order of significance of each pathway or pick up the single candidate genes or gene sets responsible for chronic graft loss, I was able to give the insight to understand the mechanisms of chronic graft loss and drug targets for preventing this graft loss. For example, I speculate that adding chemical inhibitors of specific pathways such as MAPK or JAK-STAT pathway would control the unwanted immune-related chronic graft loss.

Finally, one important question arises. Why did only R080 experience immune system activation compared with R051 despite the same immunosuppression regimen used? To find out the putative reason(s), I carefully reviewed pre-clinical symptoms, signs and laboratory data. Interestingly, I noticed that R080 had experienced two times of severe diarrhea accompanying with increases of C-reactive protein, D-dimer and serum IL-6 around DPT90 and DPT120. These findings indicated that intestinal infections were preceded to about one month before the RNA-seq sampling time and two months before the liver biopsy time. Because intestinal blood flow can directly reach to the liver via the portal vein, I hypothesized that severe intestinal infection might activate strong innate immunity and this, in turn, trigger adaptive immune response to the graft through heterologous immunity. In line with this notion, the immunologically hostile effects of infection on the transplanted allografts were well studied[93] and infection even might break down established tolerance to the graft in murine heart transplantation models[94].

There are some limitations in our work. First, I only had one monkey which

experienced relative early islet graft loss in the chronic phase after transplantation. Thus, our study cannot give a definite conclusion, but rather intriguing insight to our field. I am planning to scale up our study using more animals to validate our novel bioinformatics analysis method. Second, although I suggest that 9 pathways might have been involved in immune rejection in the chronic phase, I did not find out direct evidence that these pathways were really involved in vivo. Third, because rhesus pathways in KEGG were relatively insufficient, I was not able to analyze our data in depth. For example, even though I was interested in CD40L or IL-6 signaling pathways in our setting, I was not able to analyze them because KEGG did not support those pathways. Lastly, I was not able to pinpoint single candidate molecule or a set of molecules which can be critically responsible for graft rejection. Our next works will focus on those questions.

In conclusion, by non-invasive peripheral blood RNA-seq and innovative bioinformatics analyses, the cause of islet loss in the chronic phase after transplantation can be explored before overt graft failure.

REFERENCES

1. Morris PJ. Transplantation—a medical miracle of the 20th century. *New England Journal of Medicine.* 2004;351(26):2678-2680.
2. Abouna GM. Organ shortage crisis: problems and possible solutions. Paper presented at: Transplantation proceedings2008.
3. Cho WH, Kim SI, Kim MS, et al. A proposal to activate organ donation: report of organ allocation study group. *The Journal of the Korean Society for Transplantation.* 2009;23(1):8-14.
4. Srinivas TR, Meier-Kriesche H-U. Minimizing immunosuppression, an alternative approach to reducing side effects: objectives and interim result. *Clinical Journal of the American Society of Nephrology.* 2008;3(Supplement 2):S101-S116.
5. Tabar V, Studer L. Pluripotent stem cells in regenerative medicine: challenges and recent progress. *Nature Reviews Genetics.* 2014;15(2):82-92.
6. Ekser B, Ezzelarab M, Hara H, et al. Clinical xenotransplantation: the next medical revolution? *The lancet.* 2012;379(9816):672-683.
7. Gupta V, Sengupta M, Prakash J, Tripathy BC. Tissue Engineering and Artificial Organ. *Basic and Applied Aspects of Biotechnology*: Springer; 2017:453-474.
8. Brent L. Transplantation tolerance–a historical introduction. *Immunology.* 2016;147(3):267-268.

9. Shi Y, Inoue H, Wu JC, Yamanaka S. Induced pluripotent stem cell technology: a decade of progress. *Nature Reviews Drug Discovery.* 2016.

10. Colvin RB, Smith RN. Antibody-mediated organ-allograft rejection. *Nature Reviews Immunology.* 2005;5(10):807-817.

11. Galili U. Evolution and pathophysiology of the human natural anti-α-galactosyl IgG (anti-Gal) antibody. Paper presented at: Springer seminars in immunopathology1993.

12. Lai L, Kolber-Simonds D, Park K-W, et al. Production of α-1, 3-galactosyltransferase knockout pigs by nuclear transfer cloning. *Science.* 2002;295(5557):1089-1092.

13. Mittal S, Page S, Friend P, Sharples E, Fuggle S. De Novo Donor-Specific HLA Antibodies: Biomarkers of Pancreas Transplant Failure. *American Journal of Transplantation.* 2014;14(7):1664-1671.

14. Loupy A, Lefaucheur C, Vernerey D, et al. Complement-binding anti-HLA antibodies and kidney-allograft survival. *New England Journal of Medicine.* 2013;369(13):1215-1226.

15. Lefaucheur C, Loupy A, Hill GS, et al. Preexisting donor-specific HLA antibodies predict outcome in kidney transplantation. *Journal of the American Society of Nephrology.* 2010;21(8):1398-1406.

16. Kaneku H, O'Leary J, Banuelos N, et al. De Novo Donor-Specific HLA Antibodies Decrease Patient and Graft Survival in Liver Transplant Recipients. *American Journal of Transplantation.* 2013;13(6):1541-1548.

17. Ware AL, Malmberg E, Delgado JC, et al. The use of circulating donor specific antibody to predict biopsy diagnosis of antibody-mediated rejection and to provide prognostic value after heart transplantation in children. *The Journal of Heart and Lung Transplantation.* 2016;35(2):179-185.

18. Abbas AK, Lichtman AH, Pillai S. *Cellular and molecular immunology*. Elsevier Health Sciences; 2011.

19. Shipkova M, Wieland E. Editorial: Immune monitoring in solid organ transplantation. *Clinical biochemistry*. 2016;49(4):317-319.

20. Wood KJ, Bushell A, Hester J. Regulatory immune cells in transplantation. *Nature Reviews Immunology*. 2012;12(6):417-430.

21. Trzonkowski P, Zilvetti M, Chapman S, et al. Homeostatic Repopulation by CD28− CD8+ T Cells in Alemtuzumab-Depleted Kidney Transplant Recipients Treated With Reduced Immunosuppression. *American Journal of Transplantation.* 2008;8(2):338-347.

22. Li L, Khatri P, Sigdel TK, et al. A peripheral blood diagnostic test for acute rejection in renal transplantation. *American Journal of Transplantation.* 2012;12(10):2710-2718.

23. Khatri P, Roedder S, Kimura N, et al. A common rejection module (CRM) for acute rejection across multiple organs identifies novel therapeutics for organ transplantation. *The Journal of experimental medicine.* 2013;210(11):2205-2221.

24. Shin J, Kim J, Kim J, et al. Long-Term Control of Diabetes in

Immunosuppressed Nonhuman Primates (NHP) by the Transplantation of Adult Porcine Islets. *American Journal of Transplantation.* 2015;15(11):2837-2850.

25. Kim JM, Shin JS, Min BH, et al. Induction, management, and complications of streptozotocin-induced diabetes mellitus in rhesus monkeys. *Xenotransplantation.* 2016.

26. Buder B, Alexander M, Krishnan R, Chapman DW, Lakey JR. Encapsulated islet transplantation: strategies and clinical trials. *Immune network.* 2013;13(6):235-239.

27. Park C-G, Bottino R, Hawthorne WJ. Current status of islet xenotransplantation. *International Journal of Surgery.* 2015;23:261-266.

28. Kim S, Kim K-A, Suk K, et al. Apoptosis of human islet cells by cytokines. *Immune network.* 2012;12(3):113-117.

29. Hering BJ, Wijkstrom M, Graham ML, et al. Prolonged diabetes reversal after intraportal xenotransplantation of wild-type porcine islets in immunosuppressed nonhuman primates. *Nature medicine.* 2006;12(3):301-303.

30. Van Der Windt D, Bottino R, Casu A, et al. Long-term controlled normoglycemia in diabetic non-human primates after transplantation with hCD46 transgenic porcine islets. *American Journal of Transplantation.* 2009;9(12):2716-2726.

31. Hecht G, Eventov-Friedman S, Rosen C, et al. Embryonic pig pancreatic tissue for the treatment of diabetes in a nonhuman primate

model. *Proceedings of the National Academy of Sciences.* 2009;106(21):8659-8664.

32. Cardona K, Korbutt GS, Milas Z, et al. Long-term survival of neonatal porcine islets in nonhuman primates by targeting costimulation pathways. *Nature medicine.* 2006;12(3):304-306.

33. Cardona K, Milas Z, Strobert E, et al. Engraftment of adult porcine islet xenografts in diabetic nonhuman primates through targeting of costimulation pathways. *American Journal of Transplantation.* 2007;7(10):2260-2268.

34. Jung KC, Park C-G, Jeon YK, et al. In situ induction of dendritic cell–based T cell tolerance in humanized mice and nonhuman primates. *The Journal of experimental medicine.* 2011;208(12):2477-2488.

35. Thompson P, Badell I, Lowe M, et al. Islet Xenotransplantation Using Gal-Deficient Neonatal Donors Improves Engraftment and Function. *American Journal of Transplantation.* 2011;11(12):2593-2602.

36. Kawai T, Andrews D, Colvin RB, Sachs DH, Cosimi AB. Thromboembolic complications after treatment with monoclonal antibody against CD40 ligand. *Nat Med.* 2000;6(2):114.

37. Pitcher CJ, Hagen SI, Walker JM, et al. Development and homeostasis of T cell memory in rhesus macaque. *The Journal of Immunology.* 2002;168(1):29-43.

38. Liu J, Li H, Iampietro MJ, Barouch DH. Accelerated heterologous adenovirus prime-boost SIV vaccine in neonatal rhesus monkeys. *Journal of virology.* 2012;86(15):7829-7835.

39. Monti P, Vignali D, Piemonti L. Monitoring Inflammation, Humoral and Cell-mediated Immunity in Pancreas and Islet Transplants. *Current diabetes reviews.* 2015;11(3):135-143.

40. Kim HJ, Yoon IH, Min BH, et al. Porcine antigen-specific IFN-ɣ ELISpot as a potentially valuable tool for monitoring cellular immune responses in pig-to-non-human primate islet xenotransplantation. *Xenotransplantation.* 2016;23(4):310-319.

41. Xia H-J, Zhang G-H, Wang R-R, Zheng Y-T. The influence of age and sex on the cell counts of peripheral blood leukocyte subpopulations in Chinese rhesus macaques. *Cellular and Molecular Immunology.* 2009;6(6):433.

42. Guimond M, Veenstra RG, Grindler DJ, et al. Interleukin 7 signaling in dendritic cells regulates the homeostatic proliferation and niche size of CD4+ T cells. *Nature immunology.* 2009;10(2):149-157.

43. Ernst B, Lee D-S, Chang JM, Sprent J, Surh CD. The peptide ligands mediating positive selection in the thymus control T cell survival and homeostatic proliferation in the periphery. *Immunity.* 1999;11(2):173-181.

44. Donckier V, Craciun L, Miqueu P, et al. Expansion of memory-type CD8+ T cells correlates with the failure of early immunosuppression withdrawal after cadaver liver transplantation using high-dose ATG induction and rapamycin. *Transplantation.* 2013;96(3):306-315.

45. Ducloux D, Courivaud C, Bamoulid J, et al. Polyclonal antithymocyte globulin and cardiovascular disease in kidney transplant recipients.

Journal of the American Society of Nephrology. 2014:ASN. 2013060663.

46. Filaci G, Fenoglio D, Fravega M, et al. CD8+ CD28− T regulatory lymphocytes inhibiting T cell proliferative and cytotoxic functions infiltrate human cancers. *The Journal of Immunology.* 2007;179(7):4323-4334.

47. Ceeraz S, Hall C, Choy E, Spencer J, Corrigall V. Defective CD8+ CD28− regulatory T cell suppressor function in rheumatoid arthritis is restored by tumour necrosis factor inhibitor therapy. *Clinical & Experimental Immunology.* 2013;174(1):18-26.

48. Filaci G, Fravega M, Fenoglio D, et al. Non-antigen specific CD8+ T suppressor lymphocytes. *Clinical and experimental medicine.* 2004;4(2):86-92.

49. Ryan EA, Paty BW, Senior PA, et al. Five-year follow-up after clinical islet transplantation. *Diabetes.* 2005;54(7):2060-2069.

50. Thompson P, Badell I, Lowe M, et al. Alternative Immunomodulatory Strategies for Xenotransplantation: CD40/154 Pathway-Sparing Regimens Promote Xenograft Survival. *American Journal of Transplantation.* 2012;12(7):1765-1775.

51. Hering BJ, Cozzi E, Spizzo T, et al. First update of the International Xenotransplantation Association consensus statement on conditions for undertaking clinical trials of porcine islet products in type 1 diabetes—Executive summary. *Xenotransplantation.* 2016.

52. Heeger PS, Greenspan NS, Kuhlenschmidt S, et al. Pretransplant

frequency of donor-specific, IFN-γ-producing lymphocytes is a manifestation of immunologic memory and correlates with the risk of posttransplant rejection episodes. *The Journal of Immunology.* 1999;163(4):2267-2275.

53. Hricik DE, Rodriguez V, Riley J, et al. Enzyme Linked Immunosorbent Spot (ELISPOT) Assay for Interferon-Gamma Independently Predicts Renal Function in Kidney Transplant Recipients. *American Journal of Transplantation.* 2003;3(7):878-884.

54. Kim S, Oh E, Kim M, et al. Pretransplant donor-specific interferon-γ ELISPOT assay predicts acute rejection episodes in renal transplant recipients. Paper presented at: Transplantation proceedings2007.

55. Augustine JJ, Siu DS, Clemente MJ, Schulak JA, Heeger PS, Hricik DE. Pre-Transplant IFN-γ ELISPOTs Are Associated with Post-Transplant Renal Function in African American Renal Transplant Recipients. *American journal of transplantation.* 2005;5(8):1971-1975.

56. Poggio ED, Clemente M, Riley J, et al. Alloreactivity in renal transplant recipients with and without chronic allograft nephropathy. *Journal of the American Society of Nephrology.* 2004;15(7):1952-1960.

57. Gebauer BS, Hricik DE, Atallah A, et al. Evolution of the Enzyme-Linked Immunosorbent Spot Assay for Post-Transplant Alloreactivity as a Potentially Useful Immune Monitoring Tool. *American Journal of Transplantation.* 2002;2(9):857-866.

58. Bestard O, Crespo E, Stein M, et al. Cross-Validation of IFN-γ Elispot Assay for Measuring Alloreactive Memory/Effector T Cell Responses

in Renal Transplant Recipients. *American Journal of Transplantation.* 2013;13(7):1880-1890.

59. Ashoor I, Najafian N, Korin Y, et al. Standardization and cross validation of alloreactive IFNγ ELISPOT assays within the clinical trials in organ transplantation consortium. *American Journal of Transplantation.* 2013;13(7):1871-1879.

60. Sojka DK, Fowell DJ. Regulatory T cells inhibit acute IFN-γ synthesis without blocking T-helper cell type 1 (Th1) differentiation via a compartmentalized requirement for IL-10. *Proceedings of the National Academy of Sciences.* 2011;108(45):18336-18341.

61. Yang L, Güell M, Niu D, et al. Genome-wide inactivation of porcine endogenous retroviruses (PERVs). *Science.* 2015;350(6264):1101-1104.

62. Choi H, Lee J, Kim D, et al. Blockade of CD40–CD154 Costimulatory Pathway Promotes Long-Term Survival of Full-Thickness Porcine Corneal Grafts in Nonhuman Primates: Clinically Applicable Xenocorneal Transplantation. *American Journal of Transplantation.* 2015;15(3):628-641.

63. Mohiuddin MM, Singh AK, Corcoran PC, et al. Genetically engineered pigs and target-specific immunomodulation provide significant graft survival and hope for clinical cardiac xenotransplantation. *The Journal of thoracic and cardiovascular surgery.* 2014;148(3):1106-1114.

64. Hartig CV, Haller GW, Sachs DH, Kuhlenschmidt S, Heeger PS. Naturally developing memory T cell xenoreactivity to swine antigens

in human peripheral blood lymphocytes. *The Journal of Immunology.* 2000;164(5):2790-2796.

65. Tahara H, Ide K, Basnet N, Tanaka Y, Ohdan H. Determination of the precursor frequency and the reaction intensity of xenoreactive human T lymphocytes. *Xenotransplantation.* 2010;17(3):188-196.

66. Bachmann MF, Gallimore A, Linkert S, et al. Developmental regulation of Lck targeting to the CD8 coreceptor controls signaling in naive and memory T cells. *The Journal of experimental medicine.* 1999;189(10):1521-1530.

67. Kim S-K, Schluns KS, Lefrançois L. Induction and visualization of mucosal memory CD8 T cells following systemic virus infection. *The Journal of Immunology.* 1999;163(8):4125-4132.

68. Sprent J, Surh CD. T cell memory. *Annual review of immunology.* 2002;20(1):551-579.

69. Ware AL, Malmberg E, Delgado JC, et al. The use of circulating donor specific antibody to predict biopsy diagnosis of antibody-mediated rejection and to provide prognostic value after heart transplantation in children. *The Journal of Heart and Lung Transplantation.* 2015.

70. Li X, Ishida H, Yamaguchi Y, Tanabe K. Poor graft outcome in recipients with de novo donor-specific anti-HLA antibodies after living related kidney transplantation. *Transplant international.* 2008;21(12):1145-1152.

71. Caballero A, Fernandez N, Lavado R, Bravo M, Miranda J, Alonso A. Tolerogenic response: allorecognition pathways. *Transplant*

immunology. 2006;17(1):3-6.

72. Shapiro AJ, Lakey JR, Ryan EA, et al. Islet transplantation in seven patients with type 1 diabetes mellitus using a glucocorticoid-free immunosuppressive regimen. *New England Journal of Medicine.* 2000;343(4):230-238.

73. Barton FB, Rickels MR, Alejandro R, et al. Improvement in outcomes of clinical islet transplantation: 1999-2010. *Diabetes care.* 2012;35(7):1436-1445.

74. Fonseca SG, Gromada J, Urano F. Endoplasmic reticulum stress and pancreatic β-cell death. *Trends in Endocrinology & Metabolism.* 2011;22(7):266-274.

75. Negi S, Park SH, Jetha A, Aikin R, Tremblay M, Paraskevas S. Evidence of endoplasmic reticulum stress mediating cell death in transplanted human islets. *Cell transplantation.* 2012;21(5):889-900.

76. Lau J, Henriksnäs J, Svensson J, Carlsson P-O. Oxygenation of islets and its role in transplantation. *Current opinion in organ transplantation.* 2009;14(6):688-693.

77. Zheng X, Wang X, Ma Z, et al. Acute hypoxia induces apoptosis of pancreatic β-cell by activation of the unfolded protein response and upregulation of CHOP. *Cell death & disease.* 2012;3(6):e322.

78. Pugliese A, Reijonen HK, Nepom J, Burke GW. Recurrence of autoimmunity in pancreas transplant patients: research update. *Diabetes management.* 2011;1(2):229-238.

79. Lee Y, Ravazzola M, Park B-H, Bashmakov YK, Orci L, Unger RH.

Metabolic mechanisms of failure of intraportally transplanted pancreatic β-cells in rats role of lipotoxicity and prevention by leptin. *Diabetes.* 2007;56(9):2295-2301.

80. Leitão CB, Bernetti K, Tharavanij T, et al. Lipotoxicity and decreased islet graft survival. *Diabetes care.* 2010;33(3):658-660.

81. Barlow AD, Nicholson ML, Herbert TP. Evidence for rapamycin toxicity in pancreatic β-cells and a review of the underlying molecular mechanisms. *Diabetes.* 2013;62(8):2674-2682.

82. Drachenberg CB, Klassen DK, Weir MR, et al. ISLET CELL DAMAGE ASSOCIATED WITH TACROLIMUS AND CYCLOSPORINE: MORPHOLOGICAL FEATURES IN PANCREAS ALLOGRAFT BIOPSIES AND CLINICAL CORRELATION1. *Transplantation.* 1999;68(3):396-402.

83. Hyder A, Laue C, Schrezenmeir J. Variable responses of islet cells of different ages and species to hypoxia. Paper presented at: Transplantation proceedings1998.

84. Graham ML, Bellin MD, Papas KK, Hering BJ, Schuurman HJ. Species incompatibilities in the pig-to-macaque islet xenotransplant model affect transplant outcome: a comparison with allotransplantation. *Xenotransplantation.* 2011;18(6):328-342.

85. Jo K, Kwon H-B, Kim S. Time-series RNA-seq analysis package (TRAP) and its application to the analysis of rice, Oryza sativa L. ssp. Japonica, upon drought stress. *Methods.* 2014;67(3):364-372.

86. Kanehisa M, Goto S. KEGG: kyoto encyclopedia of genes and

genomes. *Nucleic acids research.* 2000;28(1):27-30.

87. Donato M, Xu Z, Tomoiaga A, et al. Analysis and correction of crosstalk effects in pathway analysis. *Genome research.* 2013;23(11):1885-1893.

88. Knight H, Knight MR. Abiotic stress signalling pathways: specificity and cross-talk. *Trends in plant science.* 2001;6(6):262-267.

89. Taniguchi CM, Emanuelli B, Kahn CR. Critical nodes in signalling pathways: insights into insulin action. *Nature reviews Molecular cell biology.* 2006;7(2):85-96.

90. Shannon P, Markiel A, Ozier O, et al. Cytoscape: a software environment for integrated models of biomolecular interaction networks. *Genome research.* 2003;13(11):2498-2504.

91. Najarian JS, Sutherland DE, Matas AJ, Steffes MW, Simmons RL, Goetz FC. Human islet transplantation: a preliminary report. *Transplant Proc.* Mar 1977;9(1):233-236.

92. McCall M, Shapiro AJ. Update on islet transplantation. *Cold Spring Harbor perspectives in medicine.* 2012;2(7):a007823.

93. Chong AS, Alegre M-L. The impact of infection and tissue damage in solid-organ transplantation. *Nature Reviews Immunology.* 2012;12(6):459-471.

94. Wang T, Ahmed EB, Chen L, et al. Infection with the intracellular bacterium, Listeria monocytogenes, overrides established tolerance in a mouse cardiac allograft model. *American Journal of Transplantation.* 2010;10(7):1524-1533.

국문 초록

서론: 최근 비약적인 발전을 이룬 이종췌도 전임상 이식 결과로 이종췌도이식의 임상 적용이 가까이 왔다. 임상 적용까지는 면역 억제 프로토콜의 확립이 필요한데, 이를 위해서는 이종이식편의 운명을 예측할 수 있는 면역 모니터링이 필수적이다. 하지만, 이종췌도이식 전임상 실험에서 이식편의 운명을 예측할 수 있는 면역 표지자들에 대한 보고는 매우 부족하다. 따라서, 이 논문에서는 첫 번째로, 이종췌도이식에서 이식편의 운명을 예측할 수 있는 면역 표지자를 제시하려 한다. 또한, 두 번째로 돼지 항원 특이적 세포 면역 반응을 모니터링 할 수 있는 적절한 방법을 고안하여 적용하고, 세 번째로 이식 후 만성기 췌도 소실의 원인을 규명해 보고자 하였다.

방법: 다양한 면역 억제제를 사용하여 돼지 이종췌도이식을 시행한 총 17 마리 붉은원숭이의 말초혈액단핵구를 정기적으로 분리하였다. 이 말초혈액단핵구 중 T 세포의 기능적 아형을 유세포분석기를 통해 분석하고 이식편의 생존과의 관련성을 분석하였다. 이후, 돼지췌도 특이적 인터페론 감마 엘리스팟 분석법을 셋업하고, 4 마리의 원숭이에서 시간에 따른 돼지 췌도 특이적 인터페론 감마 엘리스팟 분석을 진행하였다. 2 마리의 원숭이의 말초 혈액에서는 RNA 염기서열분석을 진행하였고, 만성기에서 상대적으

로 빠른 췌도 이식편의 소실을 보인 원숭이의 췌도 소실 원인을 다양한 생물정보학 분석을 통해 확인하였다.

결과: 토끼 항흉선세포글로불린을 이용하여 림프구를 제거한 17 마리의 원숭이개체에서 $CD3^+$ T 세포의 정상개수로의 회복은 38.2 ± 47.7 일이 소요되었다. $CD8^+CD28^-CD95^+$ 작동 기억 세포가 다른 아형 T 세포 보다 빠른 속도로 분열하였고, $CD4^+/CD8^+$ T 의 값이 초기 이식편 소실과 의미 있는 상관관계를 보였다. 한편, 2.5×10^5 개의 원숭이 말초혈액 단핵구를 5.0×10^5 개의 돼지 비장 세포를 함께 배양한 엘리스팟 분석 결과 명백한 이식편의 거부반응이 일어 난 후에, 돼지 세포 특이적으로 IFN−γ를 생산하는 세포의 증가를 확인 할 수 있었다. 생물정보학을 이용한 말초혈액 RNA 염기서열 분석 결과 만성기 췌도 이식 소실이 면역학적인 반응임을 이식편 거부 반응이 진행되는 초기 말초혈액에서 확인 할 수 있었다.

결론: $CD4^+/CD8^+$ T 세포 비율은 영장류 이종췌도이식에서 이식편의 조기 소실을 예측할 수 있는 마커로 사용할 수 있으며, 돼지 항원 특이적 IFN−γ 엘리스팟 분석법은 T 세포 의한 거부 반응을 모니터링 할 수 있는 믿을 수 있는 방법이다. 만성기 췌도 이식의 소실편은 생물정보학을 이용한 말초혈액 RNA 염기서열 분석 결과 면역학적 현상임을 거부 반응 초기의 말초혈액 샘플을 통해서 알 수 있었다.

* 본 졸업 논문의 일부는 현재 American Journal of Transplantation (Shin JS, Kim JM, Kim JS, Min BH, Kim YH, Kim HJ et at. Long-term control of diabetes in immunosuppressed nonhuman primates (NHP) by the transplantation of adult porcine islets. American Journal of Transplantation. 2015;15:2837-50), Xenotransplantation (Kim JM, Shin JS, Min BH, Kim HJ, Kim JS, Yoon IH et al. Induction, management, and complications of streptozotocin-induced diabetes mellitus in rhesus monkeys. Xenotransplantation. 2016; 23: 472-78) 그리고 Xenotransplantation (Kim HJ, Yoon IH, Min BH, Kim HY, Shin JS, Kim JM et al. Porcine antigen-specific IFN-γ ELISpot as a potentially valuable tool for monitoring cellular immune responses in pig to non-human primate islet xenotransplantation. Xenotransplantation. 2016; 23(4): 310-9) 에 출판 완료된 내용을 포함하고 있으며 Xenotransplantation (Shin JS, Ki JM, Min BH, Yoon IH, Kim HJ, Kim JS et al. Pre-clinical results in pig-to-nonhuman primate islet xenotransplantation using anti CD40 antibody based immunosuppression. Xenotransplantation. Manuscript ID: XENO-16-O-0082), Xenotransplantation (Kim HJ, Yoon IH, Kim JS, Nam HY, Min BH, Shin JS, et al. $CD4^+/CD8^+$ T cell ratio as a predictive marker for early graft failure in pig to non-human primate islet xenotransplantation with immunosuppression 그리고 Nature communications (Kim HJ, Moon JH, Shin JS, Kim B, Kim JS, Min BH et al. Bioinformatics analysis combined with peripheral blood RNA-sequencing unveiled insidious immune rejection in the chronic phase after pig-to-nonhuman primate islet xenotransplantation. 에 투고 완료 혹은 투고 예정인 내용을 포함하고 있습니다.

주요어 : 췌도 이식, 돼지의, 이종 이식, 영장류, 세포 면역 모니터링, 엘리스팟, RNA 시퀀싱, 생물정보학

학 번 : 2012-30577